Chemical Vapor Deposition

DOI: 10.1002/cvde.201300051

Review

Review of CVD Synthesis of Graphene**

By *Roberto Muñoz** and *Cristina Gómez-Aleixandre*

This article presents an overview of the research highlights in graphene synthesis by CVD. The growth mechanisms over transition metals and alloys (with emphasis on Cu and Cu alloys) are discussed, including new developments and experiments in transfer-free graphene growth on dielectric materials. The focus is on the role of the various synthesis parameters, including the thermodynamic aspects of the chemical process, and the physical, chemical, and morphological properties of the substrate catalyst. The relationships between these parameters, and the properties of the as-grown graphene are discussed. Some important relationships are reviewed and used to influence the fundamental parameters of, and methods for, the synthesis of high quality graphene.

Keywords: Graphene, Plasma, Synthesis

1. Introduction

Graphene, a two-dimensional, single-layer sheet of sp^2-hybridized carbon atoms, has attracted world-wide attention and research interest, owing to its exceptional physical properties, such as high electronic conductivity, good thermal stability, and excellent mechanical strength.[1]

Since the discovery of graphene by Novoselov,[2] the "top-down" exfoliation technique has been widely used to produce two-dimensional atomic crystals, including not only graphene but also many other 2D materials, such as BN and MoS_2.[3] This process of producing graphene sheets has been found to be reliable and easy, and has attracted the immediate attention of the scientific community. Up to now, the best quality graphene, in terms of structural integrity, has been obtained by this method, however only flat graphene flakes (tens of micrometers in size) can be produced, and the number of exfoliated layers is not easily controlled. As in most practical applications conceived for graphene, including microelectronics, optoelectronics (solar cells, touch screens, liquid crystal displays), graphene based batteries, super-capacitors, and thermal control, large area and high quality with low structural defects graphene is needed,[4] so other methods should be developed. A synthesis route using CVD could hold the answer to this complex problem.

The preparation of graphite from heterogeneous catalysis on transition metals has been known for some years. Independently of this, the first report on CVD synthesis of few-layer graphene (FLG) was published in 2006.[5] Since then, the CVD "bottom-up" synthesis has evolved to a scalable and reliable production method of large-area graphene. Synthesis of large-area and high-quality graphene has been demonstrated by this method,[6–8] however comparing the properties of CVD-produced graphene to those of exfoliated graphene, the latter continues to exhibit better quality so far.

Currently the growth and development of high-quality, large-area, CVD-produced graphene on catalytic metal substrates is a topic of both fundamental and technological interest. Since the large-scale graphene films synthesized so far have typically been polycrystalline, the research effort is aimed to control the domain size, the number of graphene layers, the density of grain boundaries, the defects, and so on. For graphene materials to realize the promise of "graphene-based applications", it is clearly necessary to solve those problems, preventing defects in fabricated devices. Preparation of large-area-domain, single-crystalline graphene has recently made great progress. Different groups have published reports on the synthesis of millimeter-size single crystals. We also summarize these new, exciting, experimental results.

There are already several and recently published comprehensive reviews dealing with the theoretical properties of graphene for electronics,[9] and also with future applications of graphene and graphene-based materials.[10–16] Among these review papers, a very recent publication by Zhang et al.[17] covers the production of graphene by CVD in a convincing way, though they do not include a detailed discussion on precursor gas decomposition kinetics as well as the role of hydrogen. This discussion is of

[*] R. Muñoz, Dr. C. Gómez-Aleixandre
Surfaces & Coatings Dept., Instituto de Ciencia de Materiales de Madrid CSIC, Madrid 28049, (Spain)
E-mail: rmunoz@icmm.csic.es

[**] The authors acknowledge the financial support from the Spanish MICINN Project No CSD2008-00023. The research leading to these results has received funding from the European Union Seventh Framework Programme under grant agreement n°604391 Graphene Flagship.

great interest for the precursor selection in low-temperature experiments using plasma-assisted techniques. The discussion about the growth of multilayer graphene on copper, widely treated in this work, was also obviated by Zhang et al. Lastly, they do not take into account either the evaporation of copper during annealing or the importance of the transfer-free graphene process when plasma-assisted techniques are used. This review includes all these aspects, and is aimed at people interested in practical questions in the field of the synthesis and catalysis of graphene and graphene-based structures.

2. CVD Synthesis and Growth of Graphene

There exist comprehensive review articles and books dealing with the generic aspects of CVD. Here we are only interested in describing elemental details of CVD applied to graphene synthesis. We encourage the readers to increase their knowledge with the fundamental aspects of vapor deposition processes revisiting the literature.[18–23]

2.1. Brief Description of CVD Chemical Reactions and Processes

CVD involves the activation of gaseous reactants and the subsequent chemical reaction, followed by the formation of a stable solid deposit over a suitable substrate. The energy that the chemical reaction demands can be supplied with the aid of various sources; heat, light, or electric discharge are used in thermal, laser-assisted, or plasma-assisted (PA) CVD, respectively.

The deposition process can include two types of reactions; homogeneous gas-phase reactions, which occur in the gas phase, and heterogeneous chemical reactions which occur on/near a heated surface leading, in each case, to the formation of powders or films.

Though CVD has been used to produce ultrafine powders, this review article is mainly concerned with the CVD of extremely thin graphene films. So heterogeneous chemical reactions should be favored and homogeneous chemical reactions avoided during the designed experiments. Figure 1 shows a schematic diagram of a typical CVD process.

2.2. Preparation of CVD-produced Graphene

The CVD of large-area, single-layer, graphene on metal films has been explored widely in some respects. Despite the significant progress, CVD-produced graphene is a polycrystalline film made of micrometer- to millimeter-size domains. To date, the graphene films grown on Ni foils or films do not yield uniform monolayer graphene**.** In most cases, a mixture of monolayer and few layers (polygraphene) are obtained. On the other hand, it was shown that Cu is an excellent candidate for making large-area, uniform thickness (95%), single-layer graphene films due to the low solubility of C in Cu.[6] It was suggested and even demonstrated that the

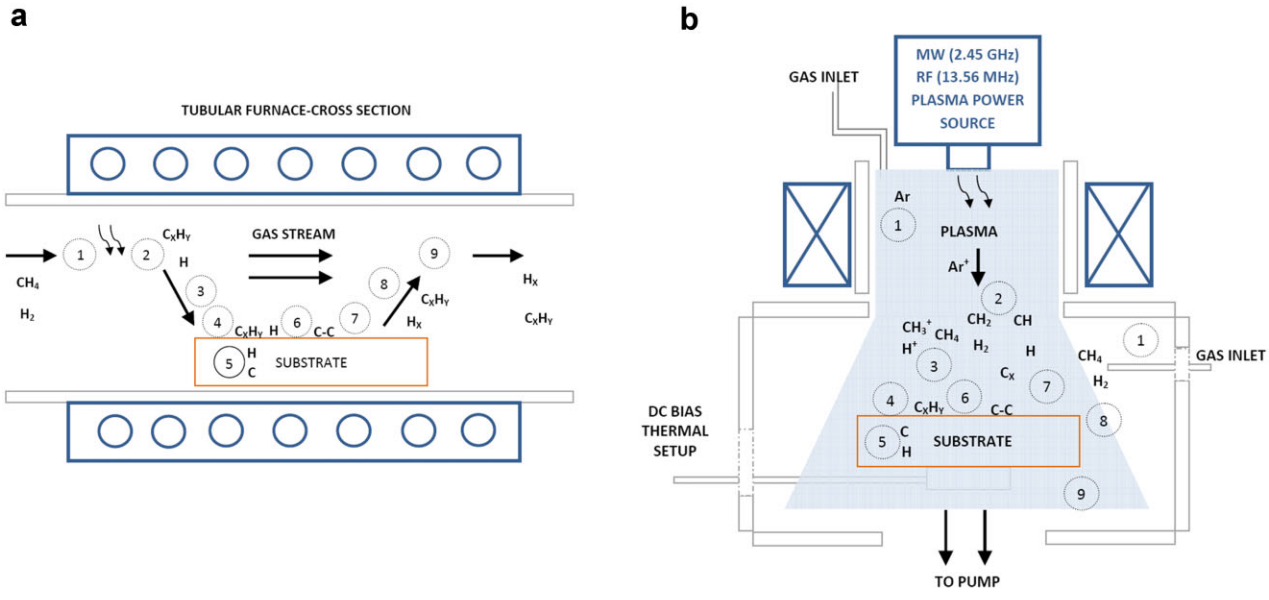

Fig. 1. Schematic diagrams of a) thermal CVD and b) plasma-assisted CVD processes in the case of graphene from CH_4/H_2 mixtures. 1. Transport of reactants by forced convection. 2. Thermal (a) or plasma (b) activation. Homogeneous gas reaction with particles and powder production should be avoided in graphene synthesis, controlling the kinetic parameters (P,T,n). 3. Transport of reactants by gas diffusion from the main gas stream through the boundary layer. 4. Adsorption of reactants on the substrate surface. 5. Dissolution and bulk diffusion of species depending on the solubility and physical properties of the substrate. 6. Thermal activation-mediated-surface processes, including chemical decomposition (catalytic), reaction, surface migration to attachment sites (such as atomic-level steps), incorporation, and other heterogeneous surface reactions. Growth of the film. 7. Desorption of by-products from the surface. 8. Transport of by-products by diffusion through the boundary layer and back to the main gas stream. 9. Transport of by-products by forced convection away from the deposition region.

graphene growth on Cu is somehow surface-mediated and self-limiting.

2.2.1. Processing Steps

From a practical point of view, some critical steps have to be taken to get exposure of the catalyst surface to the gas precursors. One prior step is substrate surface modification through cleaning processes, including chemical reduction inside the processing chamber. The detailed step-by-step process is basically as follows.

- *Heating step*: heating the catalyst-substrate (in a controlled atmosphere) and gases (in hot-wall reactors) up to the pre-process temperature.
- *Annealing step*: Maintaining the temperature and gas atmosphere so reducing the catalyst surface. This is the first chemical reaction of the whole process. It is performed to clean the catalyst surfaces and modify, as far as possible, the surface morphology including crystalline orientation, roughness (smoothing), and grain size of the metal catalyst. Metal evaporation should be avoided as much as possible.
- *Growing step*: Introduction of new precursors and growth of graphene over the catalyst substrate. During the growth process there are different strategies to grow the graphene film. There are one-step processes or many-step processes. During the steps it is possible to modify the pressure or mix of gases, residence time, temperature, gas flow, etc. It is important to take into account that, depending on the nature of the catalyst (solubility, catalytic action, and so on), the graphene may grow during this step or in the next one.
- *Cooling step*: After the growing step, the next step is cooling the reactor in a proper atmosphere. The atmosphere commonly used is similar to that of the annealing or growing step, until the reactor temperature is under 200 °C, to prevent oxidation of the catalytic surface not covered or graphene functionalization with oxygen-containing groups. When working with high solubility substrates, *cooling step dynamics are critical in controlling the growth* due to the solubility dependence.
- *Final step*: Backfill with inert gases (Ar, N) up to atmospheric pressure and open the reactor chamber.

2.2.2. Growth Kinetics and Reaction Mechanisms

Hydrocarbon-based reactants, the most mentioned being methane (CH_4), are commonly used as C source. Due to strong C-H bonds in the methane molecule (440 kJ mol^{-1}), its thermal (non-catalytic or non-plasma-activated), decomposition (step 2 in Fig. 1) occurs at very high temperatures (>1200 °C).[24] This high temperature is not easily obtained in a typical thermal CVD set-up. To reduce the temperature of the decomposition of methane, different transition metal catalysts (e.g., Fe, Co, Ni, Cu) are widely used. This catalytic behavior is observed when growing CVD-produced graphene on metals at low temperatures (<900 °C) to a greater or lesser extent. Therefore, non-catalytic activation can be considered negligible when working in thermal systems.[25] On the other hand, in the case of PACVD, the activation and decomposition of gases prior to reaching the substrate is effectively performed, but surface diffusion is a thermal-mediated process and plays a fundamental role in growth kinetics.

2.2.2.1. Growth kinetics

As the graphene synthesis process is a heterogeneous, catalytic, chemical reaction, the metal performs the two different roles of substrate and catalyst. Therefore, in a typical thermal catalytic CVD, the film grown over metal substrate reduces the catalytic activity due to catalyst poisoning. This should announce the end of the reaction and the graphene film formation. If the overall process is performed on the surface (adsorption, decomposition, and diffusion of molecules), monolayer graphene is preferentially grown. This is known as a "self-limiting" effect and has only been observed in Cu to date (and also depends on the process conditions). On Ni and other common transition metals (Co, Ru, Ir, etc.) it has been demonstrated that CVD growth of graphene occurs by carbon bulk diffusion due to the high solubility of carbon and segregation (Fig. 2) during the cooling step. In this latter case, solid solution of a mixture of elements is formed near a surface, and the resulting graphene depends on the kinetic parameters selected for the synthesis. Among all the thermodynamic parameters, a fast cooling rate seems to be a critical factor in suppressing the formation of multiple graphene layers.[25,26] A more complex deposition process results when an extra gas phase activation (decomposition by plasma or very high, >1200 °C, temperature in Fig. 2) is performed. In this case, the chemical reaction evolves to a mixture of heterogeneous catalysis and decomposition in the vapor phase. The reaction cannot then be considered as totally controlled by the catalyst.

The use of a carbon isotope-labeling technique in conjunction with Raman spectroscopic mapping demonstrated effectively the different kinetic behavior of the CVD growth of graphene on Ni and Cu.[27,28] By this technique it was possible to track carbon during the growth process. The two different mechanisms of graphene growth observed on Ni and Cu can be understood from the C-metal binary phase diagram, the most important difference being that the solubility of C in Cu is much lower than that in Ni. Only a small amount of carbon can be dissolved in Cu. The source of C is mainly CH_4 that is catalytically decomposed (dehydrogenated in Fig. 2) on the Cu surface. This route facilitates surface migration and monolayer graphene growth. Experiments with high-temperature cycles performed on graphene films of approximately 0.5 monolayer coverage on Cu while continuously imaged using low-energy electron microscopy

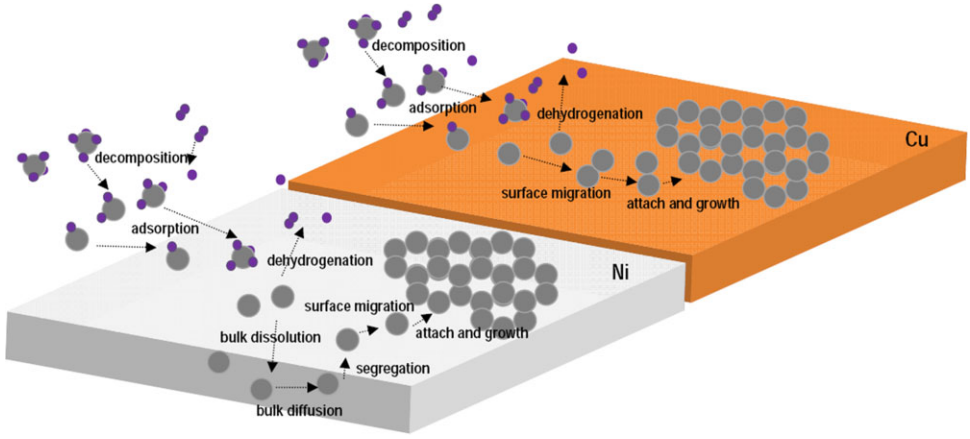

Fig. 2. Growth kinetics in CVD-produced graphene on various catalysts: Case of CH_4 on Ni and Cu.

(LEEM) confirmed this demonstration.[29] No C precipitation or island growth was observed during cooling, in agreement with preliminary reports, suggesting that the process is confined to the surface, with negligible dissolution and precipitation of C from the substrate.

In contrast, Ni can dissolve many more carbon atoms. The graphene growth comes mainly from the precipitation during the cool-down of the process, and "polygraphene" was detected in most cases. One opportunity for Ni is that the solubility and precipitation process can be controlled to some extent with the annealing, growing, and cooling rates.

It is worthy of mention that, in the case of Cu, it has been shown that the result is not always a graphene monolayer; there can also be a small fraction of flakes (few layers) stacked on the graphene film. To dispel doubts, termination of flake growth due to full coverage of the Cu surface with graphene has been observed, suggesting that the carbon species for flake growth had a similar origin to that for the first graphene layer.[30,31] One possible explanation for these small multilayer areas could be that the nature, composition, and morphology of nucleation centers have an important role in the first stage of nucleation. Also is important to note that, for the graphene layer in contact with the metal, the edge growth rate could be faster than the growth rate of the second and subsequent layers, that may be attributed to a more difficult access of the species to upper- or lower- layers.

2.2.2.2. *Reaction mechanisms*

One explanation of reaction mechanism depending on the nature of the catalyst has already been proposed, based on spectroscopic ellipsometry (SE) experiments.[32] Primarily, the difference in the growth kinetics and mechanism between Ni and Cu was ascribed to the really different carbon solubility in Cu compared to Ni. The mechanism, however, shows more complex differences. A general picture of the reaction mechanisms during synthesis is shown in Figure 3. During the annealing step, the catalyst surface is reduced by molecular hydrogen. At the end of this process, the bare metal surface also gets exposed to hydrogen, so the first step to be considered should be the dissociative chemisorption of H_2 on the metal surface, Reaction B2. Under typical conditions of graphene synthesis, this process takes place on Cu and Ni surfaces with different trends. In the case of Ni, it is more probable for hydrogen to recombine and desorb from the surface (Reactions B2, A1) but this is not directly applicable for Cu that exhibits much greater hydrogen solubility.[32,47,48] In this case, saturation would be necessary to desorb molecular hydrogen from the Cu surface. Therefore, before exposure of the catalyst to hydrocarbons, a surface and/or subsurface partially covered with atomic hydrogen could be the starting point.[46]

After exposure to hydrocarbons (diluted in molecular hydrogen in most cases), the next step to discuss is the competitive process between the dissociative chemisorption of H_2 and the physical adsorption and dehydrogenation of CH_4 on available surface sites(s) of the catalyst (Ni or Cu), according to Reactions A1-B2 and A2-B1, respectively.

During the next steps CH_x (CH_4) catalytic decomposition (dehydrogenation in Fig. 2, and Reaction B1 in Fig. 3) takes place on the metal surface. The precise moment when the precursor dehydrogenation is completed remains an open question. According to theoretical calculations based on density functional theory (DFT),[35,50,36] dehydrogenation reactions probably take place up to $x = 2$ (Fig. 3) in the case of Cu, the CH monomer dissociation being the rate-limiting step, and difficult to complete. On the other hand, complete monomer dehydrogenation and carbon bulk diffusion is expected in the case of high-solubility metals (Ni), even though CH dissociation has a high activation barrier,[49] even on steps[50] at the process temperatures. These monomers on Cu continue their path towards graphene nucleation, being dimer formation with simultaneous dehydrogenation a favorable reaction from an energetic point or view (Reaction D, Fig. 3). According to first-principles calculations within DFT,[37] CC dimers are stable on all sites on a Cu surface. Moreover, carbon dimers containing hydrogen

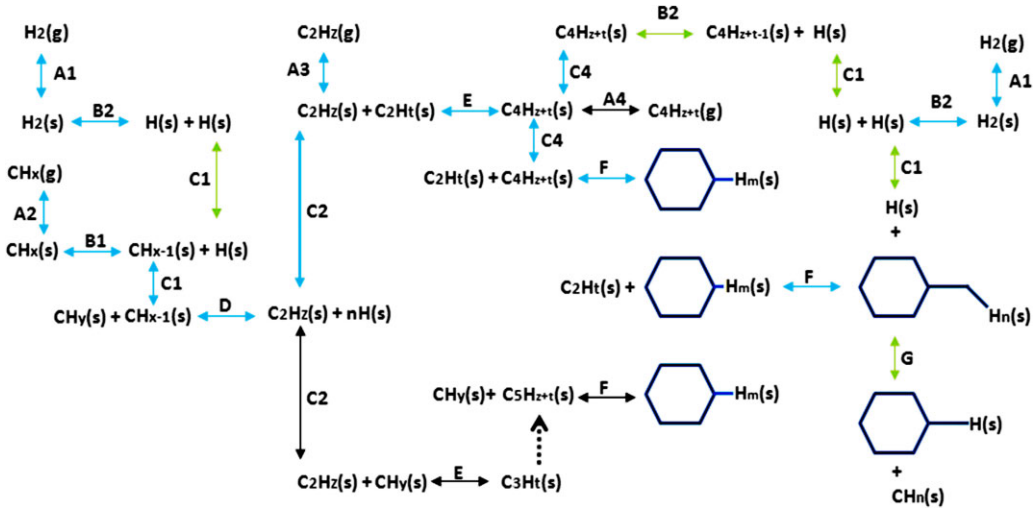

Fig. 3. Reaction mechanisms in CVD-produced graphene on transition-metal catalysts. More probable (but not unique) reaction mechanisms in blue arrows and $z, t, m = 0$. Reaction type A: adsorption-desorption. A1, A3 desorption favored by hydrogen saturation on the surface (from precursors). B: dehydrogenation-hydrogenation. Probable source for hydrogenation is molecular H_2 precursor. C: surface diffusion or migration, more favorable for dimers (C2). Dimers with high hydrogen saturation probably suffer desorption or cracking. D: dimerization with or without simultaneous dehydrogenation - (cracking) decomposition [v]. Dimers with hydrogen are not stable at high temperatures. E: polymerization - (cracking) decomposition. F: aromatization – decomposition. More stable arm-chair edges. G: decomposition of aromatics (hydrogen attack). Reactions with hydrogen in green arrows.

are very unfavorable on a surface with low adsorption energies,[39,42,43] even in defects,[44] and desorb or immediately decompose even at very low temperatures,[40,45,53] as demonstrated in temperature-programmed desorption (TPD) and thermal desorption spectroscopy (TDS) experiments.[52] Complementary studies of acetylene (CH≡CH) aromatization over transition metals also demonstrated that the benzene ring is not stable at the metallic surface.[41] Therefore, in the case of Cu, Reaction D with $z = 0$ should be considered in carbon deposition, this moment being the most probable to complete the dehydrogenation and the formation of CC bonds with sp^2-hybridization. Other routes that include carbon dimers, trimmers, and tetramers as a result of carbon atom-by-atom incorporation (Reactions E,F in black, Fig. 3) have been also studied by DFT methods.[51] Important activation barriers were involved in this reaction path due to the formation of bridging-metal (BM) structures with energy barriers higher than the diffusion barriers of dimers, and subsequent aromatization. To clarify the nucleation model on Cu (111), Riikonen et al.[38] emphasized the role of mobile carbon dimers during the growth of graphene on Cu. Several competing processes were taken into account, namely (1) dimer formation, (2) dimer migration, (3) back dissociation of dimers into individual atoms, (4) migration of carbon along the surface, and (5) migration of carbon atoms deeper into the bulk. On the basis of theoretical calculations, processes (1) and (2) were found to be dominant. In detail, it was observed that the formation of carbon dimers was exothermic, and that the migration barrier for the dimer to move on the Cu(111) surface was small ($E_a = 0.27$ eV). Once the dimer was formed, it cost more energy for the dimer to dissociate than to migrate around the surface. Riikonen et al.[38] also show how migrating dimers could form larger graphitic structures on the Cu(111) facet. Interplay of the substrate electronic states with the dimer σ_p-bonding orbital was observed; there should be an electronic factor that stabilizes the internal CC bonding of the carbon dimer, while at the same time reducing its interaction with copper. This could be an important mechanism in driving the formation of stable and mobile graphitic rings and fragments on copper. The suitable selection of thermodynamic parameters during synthesis is crucial, allowing these surface carbon species to have lower chemical potentials than carbon in the gas phase. Only in this way can carbon graphitic rings be stable at the surface, and grow into larger graphitic structures up to graphene formation.[35] Once the nucleated graphene structure is stable at the surface, further growth can be performed by attachment of carbon species onto graphene edges. Theoretical analysis of graphene-edge reconstruction showed that C insertion into the front of a growing graphene patch must depend on the edge configuration. On Cu(111), a carbon dimer has lower formation energy than a monomer. Armchair (AC) edges are also more stable than other edge possible configurations, and thus the addition of C should occur preferentially (but not only) in the form of dimers to AC edges. After a C2 dimer diffuses to an AC site and forms a hexagon on the pristine AC edge, the second hexagon then forms at an adjacent AC site by insertion of another C2 dimer.[54]

3. Towards High-quality Graphene: Effect of Experimental Parameters

CVD chemical reactions, graphene synthesis steps, and growth kinetics aspects, have just been reviewed. Growth

Table 1. Summary of selected CVD conditions reported in the literature.

References	CVD technique	P [Torr]	Gas source	Flow rate CH_4:H_2:Ar [sccm]	Substrate	t [min]	Temp [°C]	Power [kW]	Observations
6	LPCVD	0.54	CH_4:H_2	35:2	Cu	1–60	1000		
31	LPCVD	0.2–2.5	CH_4:H_2	7:2	Cu	1–60	1035		Two step process
25	APCVD	AP	CH_4:H_2	5–25:1500	Ni	5–10	900–1000		P_{CH4} = 2.53–12.46 Torr
7	LPCVD	0.460	CH_4:H_2	24:8	Cu	30	1000		P_{CH4} = 345 mTorr
121	LPCVD	0.625	CH_4:H_2	15:7	Cu	30	1000		P_{CH4} = 200 mTorr
121	APCVD	AP	CH_4:H_2:Ar	0–450:50–200:0–450	Cu	20–30	1000		Six experiments, variable flow ratio
142	LPCVD	0.45	CH_4	70	Cu	15	1000		Hydrogen depletion cooling rate 18 °C min^{-1}
130	APCVD	AP	CH_4:H_2:Ar	250:4000:1000	Ni	0.5–7	960-970		P_{CH4} = 36.2 Torr
135	SWP-CVD	3–5 Pa	CH_4:Ar:H_2	30:10:0 30:20:10	Cu, Al	0.5–3	300–400	3–4.5	
136	MWCVD	20	CH_4:H_2	1:80	Ni	1	450–750	1.4	P_{CH4} = 247 mTorr
32	LPCVD	4	CH_4:H_2:Ar	100:0–50:Ar	Ni,Cu on SiO_2/Si	1–60	900		SS CVD reactor.Ar is diluent to keep the P_{CH4} constant
109	APCVD	AP	CH_4:H_2:Ar	0.025–142: 10:600	Cu		1000		P_{CH4} = 311 mTorr–143 Torr
122	APCVD	AP	CH_4:Ar:H_2	20% CH_4 in Ar 10–50:600 H_2	Cu				P_{CH4} = 2.5–11.7 Torr
123	APCVD	AP	CH_4:Ar:H_2	5–500 ppm 1.3% H_2 F_{total} 1500sccm	Cu	5–60	1050		Two step process. P_{CH4} = 3.8–380 mTorr

kinetics and reaction paths are not completely known, and more complementary experimental work should be performed in order to understand the actual precursor decomposition routes in each case.

Concerning the synthesis of high-quality, single-crystalline, and millimeter-size graphene domains, great progress has recently been achieved. Wu et al.,[61] Yan et al.,[68] and more recently Chen et al.,[69] reported the growth of millimeter-sized graphene domains under various pressure regimes. These reports confirmed the use of Cu foils as an effective catalyst and substrate material for single-crystal graphene growth. Among the fundamental factors that influence the achievement of high-quality and large-domain synthesis, high temperature and pressure[62] during hydrogen annealing and growth, low partial pressure of the carbon precursor diluted in hydrogen at low flow rates, and long exposure times seem to be crucial. Moreover, during low pressure synthesis, evaporative loss of Cu should be suppressed.

In this section, all the mentioned parameters and other fundamental factors that could have a great influence on the high-quality synthesis of monolayer, bilayer, or FLG films will be discussed. Table 1 summarizes selected CVD conditions from among those reported in the literature.

3.1. Type of Precursor Material

Gas, liquid, and solid precursors, mainly hydrocarbons and polymers (C- and H-based compounds), have been used for graphene synthesis.[55] The fundamental question to bear in mind is that they are all suppliers of C, and just before reaching the surface they are always in the gas phase. Therefore, a critical parameter in graphene synthesis is that the energy needed to perform the whole process depends on the type of precursor.[34,36] One way to reduce this energy demand could be the use of low CH bond energy precursors, another way being the use of catalysts (not discussed in this section). Accordingly, a key parameter to take into account is the dehydrogenation energy of the precursor (CH_x to CH_{x-1}). This is a highly endothermic process in the gas phase, although on the metal surface there is a significant reduction of the energy required, owing to the presence of strong
M–CH_{x-1} and MH interactions.[36]

As we have seen above, the decomposition (dehydrogenation) in the gas phase can be performed by high temperature or plasma-assisted processes. On the other hand, when the species are adsorbed, the decomposition is a catalytic process. The gas-phase decomposition, always performed before adsorption, is widely used in typical reactions in horizontal, quartz, hot- wall CVD reactors. In some cases, however, as in CH_4 graphene synthesis, the effect of the thermal heating of the gas is negligible, so thermo-catalytic decomposition on a metal surface is crucial. Later it will be discussed that, in current experimental work, PACVD (activation of gases with electromagnetic energy) combined with thermal heating of the catalysts is being widely used. Therefore, there are two possible routes in synthesis; gas pre-activation-dissociation before reaching the substrate or only thermo-catalytic decomposition (Fig. 1).

3.1.1. Gases

3.1.1.1. Hydrocarbons

Methane (CH_4), ethylene ($CH_2=CH_2$), and acetylene (C_2H_2), with dehydrogenation energies 410 kJ mol^{-1}, 443 kJ mol^{-1}, and 506 kJ mol^{-1},[56] respectively, are being used as typical gaseous carbon precursors. The C-H bond energy is a

key parameter in the control of the decomposition temperature and energy required. Methane, the most used, is a highly stable, saturated molecule, so the dehydrogenation in the gas phase of CH_x to CH_{x-1} is highly endothermic, the calculated values being CH_3–H, 4.85 eV;CH_2–H, 5.13 eV; CH–H, 4.93 eV; C–H, 3.72 eV.[36] On the metal surface, there is a significant reduction in these values, and theoretical calculations explained that over some transition metals even exothermic dehydrogenation processes could take place.

3.1.1.2. Hydrogen content

Hydrogen (H_2) is widely used in the cleaning and crystallization of the metallic substrates (annealing step), via oxygen reduction (M_x-O, M-O_x, oxides are always present in the catalyst surface). Also molecular hydrogen (H_2), used as a diluent gas of the carbon precursor (typically CH_4, various ratios of CH_4/H_2 have been reported in the literature) undoubtedly has to play a role in the graphene CVD growth.[57] As discussed above, its interaction with the substrate could affect the subsequent CH_4 chemisorption kinetics[32], as follows:

(i) H_2 and/or atomic H could diffuse into the catalyst depending on the solubility (metals of high hydrogen solubility and low surface diffusion), and compete with CH_4 for the initial physical adsorption;
(ii) atomic H could create sites for sticking hydrocarbon and carbon radicals on the surface by subsequent H-abstraction reactions, removing hydrogen from the surface;
(iii) hydrogen could passivate defects and grain boundaries that were believed to be nucleation sites;
(iv) atomic hydrogen could be active in the competition of CH_x deposition or C-etching; and
(v) it could play an important role in the C sp^3 to sp^2 transition.

An indication of the important role of hydrogen in determining the graphene growth kinetics and in limiting the graphene thickness comes from previous observations, such as when the fraction of CH_4 with respect to H_2 is increased, the graphene growth on Cu is no longer self-limiting.[58] The contrary, however, has also been published (dependent upon other synthesis conditions).[59]

Another question that it is worth emphasizing is the differences detected on the role played by hydrogen during the pre-treatment and the whole process, depends upon the metal used (Cu or Ni). As an example, a reversible phenomenon with respect to hydrogen for Cu was observed. Hydrogen readily bulk-diffuses into Cu, and it out-diffuses to a surface when hydrogen is turned off and pressure decreased, but it does not desorb from the surface, unlike Ni. This is consistent with hydrogen having different diffusion coefficients in Cu and Ni. At the typical growth temperature of graphene by CVD of approximately 900 °C, the in-diffusion coefficient of hydrogen in Cu is approximately one order of magnitude higher than for Ni, implying a lower hydrogen solubility in Ni than in Cu.[33] Therefore, the reaction $H(s) + H(s) \rightarrow H_2(g) + 2(s)$ is highly favored for Ni but not for Cu. So the role of hydrogen and its benefits or disadvantages during growth remains an open question.

3.1.2. Liquids

A recent publication reported the use of toluene and low pressure (LP) CVD to grow continuous monolayer graphene films at 500 °C to 600 °C on flat and electropolished Cu foils (after annealing at 980 °C).[64] The consideration that motivated the choice of toluene, along with the fact that it is considerably less toxic than others such as benzene, was actually its weak bonds. In this work, the results about the rectangular-shaped graphene domains should be particularly highlighted. The authors related it to the partial pressure of hydrogen in the reactor. Comparing the partial pressure of hydrogen reported in the literature and in these results, the higher the partial pressure of hydrogen, the more easily the domain shapes tend to an equiaxial shape due to more sharp edges and corners of the graphene flakes being etched. This means that sharp four- or six-lobe domains can grow under a lower partial pressure of hydrogen, and the hexagonal domains under a higher hydrogen partial pressure. The partial pressure of hydrogen for growing the rectangular domains that have been observed was in between these limits.

3.1.3. Solids

Many experimental works dealing with the use of solid precursors in graphene synthesis have been published. It has been demonstrated that large-area, high-quality graphene can be grown from solids. Among the precursors used are polymer films, small molecules, evaporated solids, etc. Interestingly, even food, insects, and waste have been used as a solid carbon source to generate high-quality, monolayer graphene.[60]

A first approach was the use of a solid polymer (polystyrene) as the carbon source because of its relatively weak C-H bonds and low decomposition temperature.[61] The C-H bond in polystyrene is comparatively weak, with a bond energy in the range 292–305 kJ mol^{-1}, much lower than that in typical gaseous carbon precursors such as methane (410 kJ mol^{-1}), ethylene (443 kJ mol^{-1}), and ethyne (506 kJ mol^{-1}). Varying H_2 flow and heating polystyrene (Fig. 4a) up to 215 °C (T_p in Figs. 4 and 5), it is possible to grow hexagonal graphene domains (up to 1.2 mm, breaking the thermodynamic equilibrium under suitable conditions, see Fig. 5) with low nucleation density 100 n cm^{-2} in APCVD.

Another example dealing with spin-coated poly(methyl methacrylate) (PMMA) and small molecules (fluorene ($C_{13}H_{10}$) and sucrose, table sugar, $C_{12}H_{22}O_{11}$) deposited

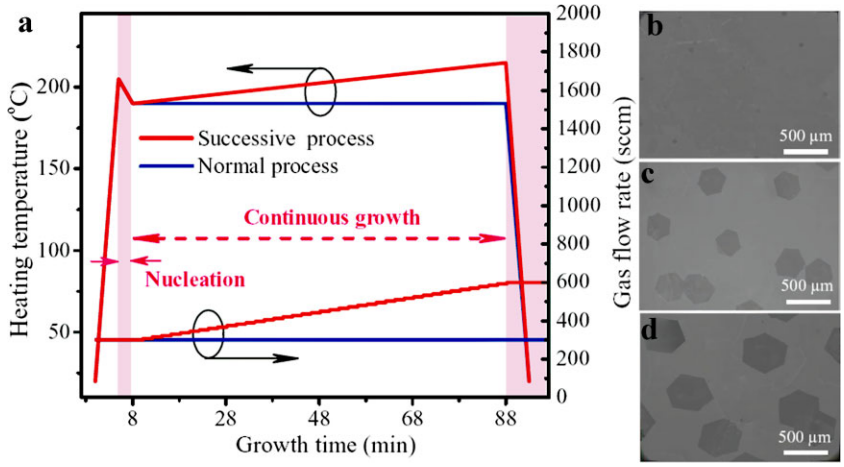

Fig. 4. a) APCVD growth of graphene at 1050 °C with a linear increase of T_p (up to 215 °C) and total reactant gas flow rate. b) SEM image of graphene nucleation sites. c) SEM image of hexagon-shaped graphene under normal growth process for 40 min. d) SEM image of hexagon-shaped graphene under continuous growth process for 40 min. Reproduced with permission [61]. Copyright 2012, Wiley-VCH Verlag GmbH & Co.

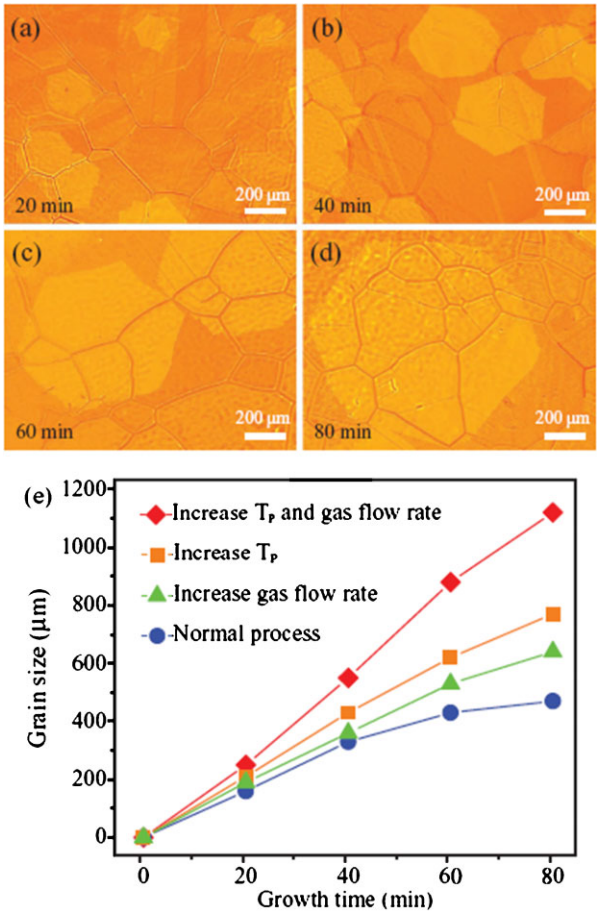

Fig. 5. Optical images of hexagonal graphene grain synthesized for a) 20 min, b) 40 min, c) 60 min, and d) 80 min. The winkle-like structures in (a–d) are grain boundaries of the copper substrate. e) The grain size as a function of growth time under different processes. Reproduced with permission [61]. Copyright 2012, Wiley-VCH Verlag GmbH & Co.

on Cu at temperatures from 800 °C to 1000 °C under LPCVD conditions have been reported.[55] It was found that the thickness of PMMA-derived graphene can be controlled (to give a monolayer, a bilayer, or a few layers) by changing the diluent gas flow rate. In the case of small molecules, although they contain potential topological-defect generators (the five-membered ring in fluorene) or high concentrations of heteroatoms (oxygen in sucrose), they also produce high-quality pristine graphene.[55] Other substrates (such as Ni, Si(100) with native oxide, and 200 nm thick SiO_2 thermally grown) were also tested. The Raman spectra confirm that Ni is an efficient catalytic substrate that converts PMMA into highly crystalline graphene. Under the same growth conditions, neither graphene nor amorphous carbon was obtained on Si or SiO_2 substrates.

Also, Hofrichter et al. published results on the fabrication of graphene on silicon dioxide by solid-state dissolution of an overlying stack of a silicon carbide layer (50 nm) and a nickel thin film (500 nm).[62] The carbon dissolves in the nickel by rapid thermal annealing. Upon cooling, the carbon segregates to the nickel surface forming a graphene layer over the entire nickel surface. By wet etching of the nickel layer, the graphene layer was allowed to settle on the original substrate. The SiO_2/Si substrate was annealed at 1100 °C, 30 s in nitrogen. When cooled, the carbon segregates to the interface forming a graphene layer, resulting in a few layer and monolayer mix (polygraphene). Further optimization to obtain a larger monolayer coverage should be possible via carefully tuning the ratio of SiC to Ni film thickness, in conjunction with an optimized cooling rate.[63]

Homogeneous single-layer graphene can be grown by simply annealing crystalline Cu(111)/c-plane sapphire at 900 and 1000 °C, due to graphitization of amorphous carbon previously deposited on the surface or coming from desorption at the furnace walls.[65] The published results confirm, however, that only if sufficient carbon source is

supplied can graphene be formed, irrespective of growth temperature (800–1000 °C) and the nature of the metal, suggesting that the carbon supply is an important factor influencing graphene nucleation. Hence, surface-induced graphitization has not proved suitable for the synthesis of high-quality material.

3.2. Substrate

Since the metal exerts a key role, as the catalyst, in the formation of graphene layers, in this section we take a look at the critical issues concerning the substrate material. The chemical and physical properties, crystallography, and morphology of the catalyst are reviewed. We address the differences due to the metallic or dielectric character of the substrates.

3.2.1. Materials

3.2.1.1. Transition metals

The formation of FLG resulting from industrial heterogeneous catalysis on transition metal surfaces has been known for years. The catalytic power of transition metals and some of their compounds is well known, and arises from their partially filled d-orbitals or from the formation of intermediate compounds that favors the reactivity of the precursor gases. Therefore, catalysis by metals results from their ability to provide low activation energy pathways for reactions, either by the facile change of oxidation states or the formation of intermediate compounds.

The CVD method on transition metals, such as Ni,[66] Pd,[67] Ru,[70] Ir,[70] and Cu[6] foils or evaporated films, revealed that the properties of the as-grown graphene films, such as quality, continuity, and layer number distribution, are dependent on the catalyst used. The different catalytic activity and solubility were seen to lead to different growth mechanisms.

Catalytic activity is related to the decomposition of hydrocarbons on metals, which produces active carbon species, and is a critical step in lowering the activation energy for the decomposition of precursor gases. As an example, the fact that graphene can grow on Pt at a relatively low temperature (750 °C) indicates that Pt has a stronger catalytic ability for CH_4 dissociation than Cu,[71] which is consistent with reported theoretical calculations.[36] Pt also has a much stronger catalytic ability for H_2 dissociation to form active atomic H. Also, the lower activity of Cu compared to Ni and other transition metals in the catalytic dissociative chemisorptions of CH_4 can be rationalized considering that it occurs by the electron transfer from the CH bonds to the 3d orbitals of the catalysts, with Ni having two 3d unpaired electrons and Cu having only one unpaired electron available for the interaction (Cu has an electron configuration $[Ar]3d^{10}4s^1$, since an electron passes from the 4d-orbital to 3d to generate a filled 3d electron shell, which is the most stable configuration).[32] Copper has not been observed to form any carbide phases, so the low reactivity with carbon could be attributed to the fact that copper has a filled 3d-electron shell, the most stable configuration (along with the half filling $3d^5$) because the electron distribution is symmetrical which minimizes reciprocal repulsions.[30]

The carbon solubility was also revealed as a key parameter in the control of the growth of graphene over metals. Various growth kinetics have been proposed, depending on the solubility of the catalyst. The growth conditions also determine the deposition mechanism defining the morphology (domain size and boundaries) and thickness of the graphene films. For example, Cu has very low carbon solubility (0.001–0.008 wt.-% at 1084 °C) compared to Co (0.9 wt.-% at 1320 °C) and Ni (0.6 wt.-% at 1326 °C). As a result of this low solubility and low catalytic activity, Cu can only form soft bonds with carbon via charge transfer from the π electrons in the sp^2-hybridized carbon to the empty 4s states of copper.[14,71,72] This combination of very low affinity between carbon and copper, along with the ability to form intermediate soft bonds, could facilitate graphitic carbon formation.

Previous results of growth on polycrystalline Ni[66,74,75] and Cu[6] substrates triggered interest in graphene synthesis by CVD for large-area deposition. In the case of Ni, the fundamental limitation was that polygraphene was mainly obtained. This lack of control over the number of layers was partially attributed to the fact that the segregation of carbon from the metal carbide upon cooling, due to high solubility (~0.6%), occurred at different rates within the Ni grains and at the grain boundaries.[73] There are some reports[63] of graphene films composed mostly of one or two layers of graphene grown by controlled carbon precipitation on the surface of polycrystalline Ni thin films during APCVD. Controlling both the methane concentration and the substrate cooling rate during growth can significantly improve the thickness uniformity.

In contrast to Ni, uniform deposition of high-quality, single layered graphene over large areas was recently achieved on polycrystalline copper foils.[6] The initial[6] and subsequent follow-on[7] studies demonstrated the growth of single-layered graphene over areas as large as 30" with 95% coverage of monolayer graphene. CVD growth of graphene on Cu is generally attributed to the thermal decomposition of hydrocarbons on the surface and the subsequent surface diffusion of carbon atoms due to the low solubility of carbon (<0.001 at.-%) in Cu. Furthermore, thin copper foils are inexpensive and can be easily etched with solvents available in most laboratories, so that transfer onto desired substrates can be readily achieved.

A recent publication claimed the growth of millimeter-sized, hexagonal, single-crystal graphene flakes and graphene films on single-crystal and polycrystalline Pt by APCVD (Fig. 6).[71] In this case, a single-crystal Pt substrate showed similar growth behavior for graphene as that on

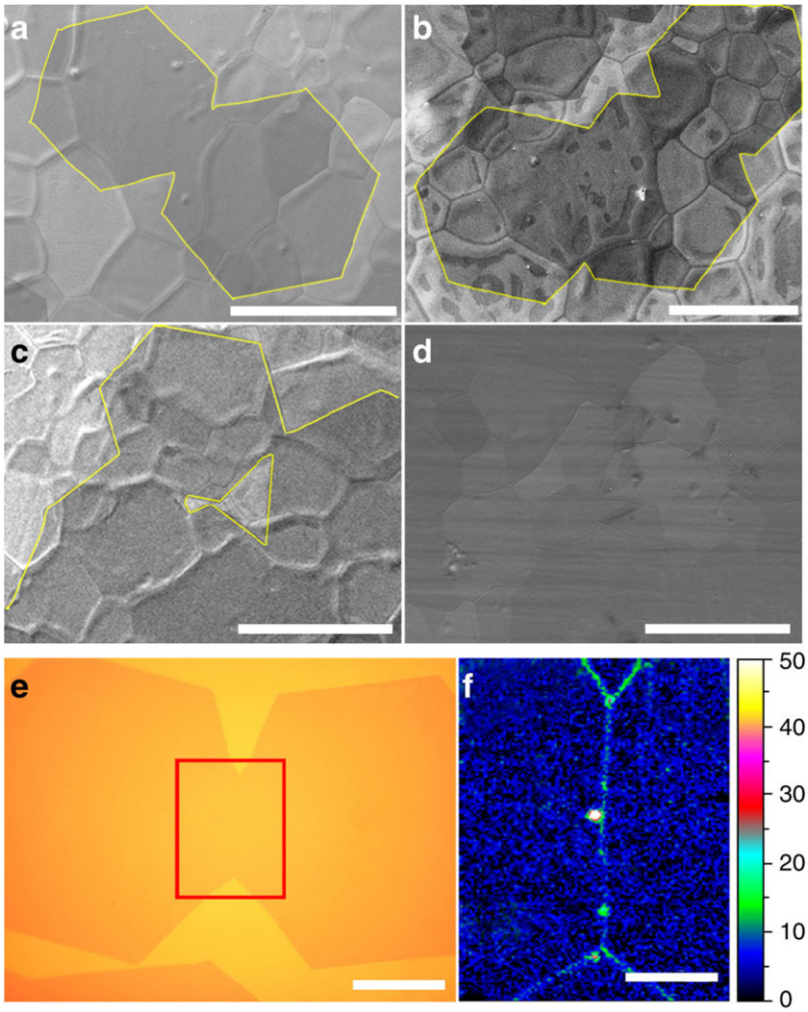

Fig. 6. Coalescence of graphene grains. SEM images of the coalescence of different graphene grains; a) two, b) three, c) many, and d) continuous graphene film formed from grains. The graphene film completely covers the Pt substrates without any gaps. e) Optical image of two coalesced graphene grains. f) Raman mapping of the intensity of the D band (1,300–1,400 cm^{-1}) at the joint area of the two coalesced grains indicated by a red box in (e). The strong intensities along the line in the mapping indicate a grain boundary. The scale bars in (a–d) are 400 μm, in (e) 50 μm, and in (f) 20 μm. Reproduced with permission [71]. Copyright 2012, Macmillan Publishers Ltd.

polycrystalline Pt. Solubility of carbon in Pt is high, 0.9 wt.-%, so a growth temperature of less than 800 °C was enough for graphene nucleation. Low CH_4 concentration was used because the size of the graphene grains was related to this parameter. Single-crystal grains of a perfect hexagon shape, with very smooth edges and lateral size of up to 1.3 mm, were obtained at 1040 °C.

Compared to Cu or Ni catalyst systems, Fe is favorable in terms of low cost, however there have been only a few studies in this area, most likely due to the complex FeC phase diagram that also offers great versatility.[76] Lowering T^a below 912 °C results in a phase transformation of the Fe-C binary mixture to body-centered cubic α-ferrite and a decrease in the solubility of C, due to the eutectic phase formation at 727 °C with a very small solubility of about 0.022 wt.-%. In this case, FLG have been grown by APCVD with CH_4. The layer number distribution was tuned by varying the procedure of the heating/cooling temperatures, cooling rate, and CH_4 flow rate.

Metal-catalyzed crystallization of a-C to graphene by thermal annealing (deposition of a layer of a-C, 2.5–40 nm thick by electron-beam evaporation on Si/SiO_2 substrates, followed by nickel or cobalt metal thin film, 100–300 nm deposition) was also performed.[77] These samples were annealed at 650–950 °C using a tube furnace under argon flow.

In conclusion, up to now the best approach to control the number of layers via metal catalysis was by a monolayer growth on very low solubility metal, such as Cu, since it has been quite difficult to control the growth of monolayer graphene via fast cooling processes on high solubility metals (Ni). Also observed was a lack of control in growing bilayer graphene, which is actually important because bilayer films seem to be the most useful in electronic applications.

3.2.1.2. Metal Alloys - Cu-Ni

Recently, more experimental efforts have been made with the intention of controlling the number of layers of nucleated graphene films; this would be a real breakthrough. Thin Ni films and fast-cooling processes have been used to hinder carbon precipitation. Not uniform graphene but polygraphene with only monolayer regions and a wide range of thicknesses has been grown by these methods. It was widely observed that monolayer graphene grows on the "flat" dimension boundaries of the metal grains, while multilayer graphene ($n > 3$) preferentially forms at the metal grain boundaries. This lack of control was the main reason for studying the growth of graphene on metal alloys.

Since Cu and Ni are well-known binary isomorphous systems, CuNi alloy is an ideal system since it has moderate as well as controllable carbon solubility by tuning the atomic fraction of Ni in Cu. To elucidate the behavior of these binary systems, Robinson et al.,[79] studied CuNi foils (90:10 by mass) from the catalyst point of view. Ni surfaces are more catalytically active than Cu surfaces, so the rate of dissociation of the hydrocarbon precursor should be much higher on the alloy than on pure Cu surfaces. In principle, this could mean lower graphene growth temperatures. Nevertheless, relatively small, 100 μm, substrate grains have been observed for the 90:10 CuNi foils annealed at 1050 °C. Therefore, either much longer annealing times or higher annealing temperatures are needed to grow centimeter-sized substrate grains. In addition, an experimental study of the equilibrium surface composition of CuNi alloy substrates by Sakurai et al.[80] found strong Ni segregation for Cu-rich alloys, which may further enhance the catalytic activity.

Growing experiments with various atomic fractions were also performed. A cold-wall chamber (8 Torr pressure and 100% CH_4) was used to obtain monolayer, bilayer, and multilayer graphene, as well as ultrathin graphite, on commercial polycrystalline CuNi (31.00% Ni, 67.80% Cu).[78] In this case, the foil showed millimeter-size grains after annealing. Various cooling rates (5 or 100 °C s^{-1}) and temperatures (930 °C to 1030 °C) were used. The observed uniformity of monolayer graphene on this CuNi alloy surface was much better than the results on polycrystalline Ni reported up to now.

Liu et al.[81] reported a facile segregation approach for this purpose using CuNi mixtures with various percentages. Bulk nickel generally contains a trace amount of carbon species, which can be brought into the thin Ni film during electron beam deposition. A sandwiched structure was grown of Cu(370 nm)/Ni(20–130 nm)(C)/SiO_2/Si, where the Ni layer was used as the carbon source (carbon content about 2.6 at.-%) and the Cu layer was employed as a favorable segregation medium. To date over 95% monolayer and 91% bilayer graphene films have been prepared by only changing the atomic percentage of Ni in the CuNi alloy. For a CuNi alloy having 5.5% Ni component, monolayer graphene occupied over 95% of the whole film. When the Ni component in the alloy was increased to 10.4%, the segregated film was dominated by bilayer graphene over 89%. Further increasing the Ni percentage leads to thicker graphene.

3.2.1.3. Metal Alloys - Ni-Au

One more novel experiment was performed by Weatherup et al.[82] This group was working on the design of alloy catalysts for low-temperature synthesis of graphene. They showed that alloying polycrystalline Ni with Au (Ni films ~550 nm thick on SiO_2(300 nm)/Si substrates covered with various thicknesses of thermally evaporated Au up to 10 nm) allows FLG with reasonable crystallinity and domain sizes to be produced by CVD at a temperature of 450 °C. This low temperature would be compatible with back-end CMOS integration. Scalable APCVD of predominantly monolayer (74%) graphene films with an average D/G Raman peaks ratio of 0.24, and domain sizes in excess of 220 μm^2, have been demonstrated. The Au alloying thereby drastically lowered the graphene nucleation density, allowing more uniform and controlled growth, and highlighting the role of step edges. The authors also found that 3–5 nm Au gave the best graphene uniformity with regards to their CVD reference conditions, with thicker Au layers leading to more inhomogeneous graphene layers.[82] One drawback could be the pre-annealing that should be applied at higher temperatures to mix the alloy, although one advantage could be that mixing can be promoted by metal co-deposition.

3.2.1.4. Dielectric substrates

Generally, CVD-produced graphene is transferred onto a desired substrate for further applications. Thus, it is of great interest to directly prepare continuous graphene films on dielectric substrates such as BN, Si, SiO_2, Al_2O_3, GaN, MgO, Si_3N_4, and so on. Considerable efforts were made to directly grow graphene films on these substrates,[83–88] but so far continuous and highly conductive films have been very difficult to synthesize. Important applications have been reported for the replacement for graphene films of conventional transparent conductive films (TCFs), including In_2O_3:Sn (ITO), SnO_2:F (FTO), and so on, however the highest efficiency achieved in solar cells was only 4.17%,[89] which can still not compete with conventional solar cells.

There are some examples of experimental work on the synthesis of graphene over dielectric substrates. Bi et al.[90] reported the direct growth of graphene films on dielectric substrates by APCVD at 1100–1200 °C using a gas mixture of CH_4, H_2, and Ar. It is important to mention that at 1200 °C, over BN, Si, SiO_2, and AlN substrates, it was not monolayer but FLG growth that was reported.

Another singular approach was the direct CVD of a single-layer or FLG film on dielectric surfaces via a sacrificial copper film reported by Ismach et al.[91] Working on the CVD growth of graphene on micrometer-thick copper foils

they noticed that a significant amount of the copper evaporated and deposited at the edges of the fused silica tube used in the CVD. Considering the melting temperature of the copper, ~1084 °C, along with the high temperature during the growth, ~1000 °C, and the low pressure in the chamber, 100–500 mTorr, the significant evaporation of the metal is not surprising. They proposed that, if long processing times are used (up to 300 min), the Cu film can evaporate completely. This CVD-produced FLG exhibits characteristics similar to those of turbostratic graphene, that is, lack of long order in the perpendicular direction. The results showed that the continuity of the metal film on the surface depends on its thickness, the metal-dielectric wetting properties, and the heating temperature and time. Typically, 100 to 450 nm thick Cu films on quartz and other insulating substrates have been used. After the initial heating, the dewetting and evaporation rates of the metal decreased, presumably due to the graphene growth that increases the coverage of the copper surface. Single-layer to FLG film was obtained, but the film was highly defective and composed of thicker, graphitic-like material and highly damaged graphene layers.

In conclusion, up to now many approaches to control the number of layers via metal alloy catalysis have been performed. There have been some important advances on this subject, with controlled few-layers growth over alloy catalysts. Nevertheless, the physical, optical, and electronic properties of these films still have to be essentially improved. Also it would be highly desirable to directly growth graphene layers on dielectric substrates. More experimental work should be performed in these areas for graphene to be competitive in practical applications.

3.2.2. Crystallographic Structure of the Metal Surface

In choosing the catalyst, parameters other than the material or chemical nature have to be taken into account. Crystal structure, texture, mono- and polycrystalline character, and the evolution of the surface morphology during synthesis have, among others, been demonstrated to be critical aspects for graphene nucleation and growth.

3.2.2.1. Single crystals, polycrystals, and grain size

There are examples of experiments where, even on a single metal grain (single-crystal), different orientations of graphene domains have been observed.[92] Moreover, in a recent work by Gao et al.[71], it was observed that a single-crystal Pt substrate showed similar growth behavior for graphene as that on polycrystalline Pt. Nevertheless, the size and orientation of the metal substrate grains were expected to have a large impact on the defect density of the graphene films grown by the dissociation of hydrocarbon molecules on metal substrates. The larger the grain size the higher-quality graphene films have been produced.[7]

3.2.2.2. Crystal structure orientation, texture, and lattice match

Graphene has a hexagonal-honeycomb lattice character. Regardless of the fact that graphene can grow on several hexagonal or other crystallographic surfaces, growth on hexagonal substrates has frequently been referred to as "epitaxial", even if a lattice match was absent between the graphene and the substrate. Lattice mismatch of less than 1% is present on Co(0001) and Ni(111) surfaces. In contrast, lattice mismatch between graphene and Cu(111), Pt(111), Pd(111), Ru(111), and Ir(111) is >1%.[14] For systems with only a small lattice mismatch, a strong interaction can result in a pseudomorphic growth resulting in a large coincidence lattice and a "Moiré pattern" type of growth as a result of different rotational alignments.[94]

In the case of copper, the role of Cu orientation and lattice mismatch was also more important than expected after the preliminary, successful, experimental results on a polycrystalline Cu(100) foil surface.[6] A detailed study of the as-grown graphene showed that the graphene had distinctive four-lobed islands and substantial in-plane rotational disorder.[29] The in-plane orientations were around two crystallographically equivalent Cu directions, a consequence of placing the six-fold graphene on the four-fold Cu(100) substrate. Furthermore, each nucleation site typically generated four graphene crystals, each with a different in-plane orientation. Island morphology was strongly determined by substrate temperature.

More recent works demonstrated that although Moiré patterns have been observed on both Cu(111)[93] and Cu(100),[65] the hexagonal lattice of Cu(111) favored the high quality of as-grown graphene. Two predominant Moiré patterns in Cu(111) were observed, which could suggest that the graphene had preferred orientations with the underlying Cu(111). The results of comparing the different orientations led to speculation that graphene would prefer nucleation on a Cu(111) crystal plane rather than on Cu(100) and (110), because of the similar crystallographic geometry in Cu(111) reducing the nucleation barrier, since the lattice mismatch between graphene and the underlying metal causes an additional energy cost.

Zhao et al.[94] also investigated the influence of the surface structure of single Cu crystals in UHV from ethylene at 900 °C. The over-coated graphene had a hexagonal superstructure (Moiré) on Cu(111), and linear superstructure with a periodicity of 11 Å and an angle of 0° on a Cu(100) square lattice. The graphene film properties have been confirmed to be much poorer on the Cu(100) surface when compared to the Cu(111) surface.

Wood et al.,[95] using different characterization techniques, found that substrate crystallography affects graphene growth even more than facet roughness. They determined that (111)-containing facets produce pristine monolayer graphene with higher quality and growth rate than (100)-containing facets, especially on Cu(100). This could be attributed to the high diffusion[93,94] and improved

adsorption of carbon-containing species on Cu(111).[96] Since Cu(111) is the lowest-energy Cu surface,[97] longer pre-growth annealing treatments under Ar/H_2 flow at 900 °C could help in the production of Cu(111) facets on the polycrystalline Cu substrate. Therefore, engineering Cu to have (111) surfaces is expected to cause monolayer, uniform graphene growth.

Recently, "orientation-controlled growth of graphene" was performed by an epitaxial CVD approach using heteroepitaxial Co,[98] Ni,[99] Cu,[100,101] Ir,[102] and Ru[103,104] films deposited on single-crystal sapphire (α-Al_2O_3(0001)) or MgO(111) substrates. This approach gave, as a result, crystalline metal films suitable for large-area graphene growth at a much lower cost than using single crystals, not only for a low carbon-solubility metal like Cu, but also for Co and Ni whose carbon solubility is high. Ogawa el al.[105] compared the domain structures of large-area, single-layer graphene films grown on heteroepitaxial Cu(111) and (100) films, both deposited by magnetron sputtering on single-crystal MgO(111) and (100) substrates, respectively. It was demonstrated that domain structure and size, as well as the orientation, were strongly influenced by the Cu crystalline plane, and that the Cu(111) was preferable for the orientation-controlled graphene growth. Graphene was epitaxially formed on Cu(111)/MgO(111) but graphene/Cu(100)/MgO(100) showed a more complex low-energy electron diffraction (LEED) pattern where graphene covered the Cu surface, with two preferential (10) orientations with angles of $0 \pm 2°$ and $30 \pm 2°$ with respect to the underlying Cu(011) lattice. Low-energy electron microscopy (LEEM) measurements for the as-grown, single-layer graphene on Cu(100) also showed that the as-grown graphene possessed a clear multi-domain structure with patches of small domains.

In conclusion, it is worth mentioning that, even though in some experiments different orientations of graphene domains on a single metal grain have been obtained, the hexagonal lattice of Cu(111) favored the high quality of as-grown graphene. Moreover, during the CVD heteroepitaxial growth on Cu(111), the orientation of graphene nuclei became well controlled, with domain boundaries atomically connected. This could represent a new alternative. Therefore, it would be advantageous to develop techniques for producing foils of these materials with a (111) surface texture.

3.2.3. Thickness, Roughness, and Morphology

3.2.3.1. Thin films and foils

Standard processes in Si technology include, among others, the deposition of Cu and Ni thin films on Si substrates and wafers. The evaporation of metals is performed in HV systems, and is not a cheap process to manage in laboratory research. Therefore, a lot of laboratory research in graphene synthesis has been performed using various catalyst configurations as thin foils (up to 25–30 μm thick). These foils were cheaper than film deposition processes, and all the processes developed on foils can be translated easily to thin films and their standard processes. Another advantage is that foils are flexible, and even though they initially have high roughness, it is also well known that annealing the foil metal can lead to a very large grain size, with a flattened surface that rivals or even exceeds the flat surfaces typically obtained by cutting and polishing single crystals. After a typical annealing process, the spaces between single atomic steps in the case of Cu are often greater than 100 nm, indicating a surface normal less than 0.1° from the (100) azimuth.[29]

It is worthy of mention that the lateral dimensions of the Cu grain boundaries have been observed to vary with the annealing pre-treatment time and also with the Cu foil thickness.[14] H_2 embrittlement of Cu could also limit diffusion, and minimizes grain growth during annealing. In this connection, the pioneering work of large-area graphene growth on Cu foils,[6,31,59] developed in LPCVD at 1000 °C from CH_4 and H_2 mixtures on foils of various thickness (12.5, 25, 50 μm) to check precipitation mechanism, did not show evidence of differences in graphene quality. Moreover, the cheap copper foils proved to be ideal for large-area graphene synthesis, up to 30" has been demonstrated.[7] On the other hand, it is commonly accepted that commercial Cu foils are (100) textured after annealing (and due to the cool rolling fabrication process) and, as seen above, the crystallography strongly affects the graphene growth. Pre-growth LEED analysis of the Cu surface also showed that annealing resulted in a (100) texture in the foil plane.[29]

Returning again to standard processes, in high performance electronic devices, the graphene must be electrically isolated from its surrounding environment. In the case of copper, this is generally achieved by etching the underlying metal substrate, with subsequent transfer to an insulating substrate, such as silicon oxide.[6] Such a layer transfer process is, however, non-ideal for nano-electronic applications due to microcracking and the potential for interfacial contamination between the graphene and the substrate. Levendorf et al.[106] demonstrated a transfer-free process for fabrication of CVD-produced graphene transistors. Instead of utilizing a bulk copper substrate, an evaporated copper film on an oxidized silicon wafer was grown. One problem with the evaporated $Cu/SiO_2/Si$ system was that, although stable at temperatures <800 °C, it was unstable at the temperature used in the synthesis. One approach to ensuring stability at the Cu/SiO_2 interface could be to minimize the graphene synthesis temperature. Another approach presented evidence of significant Cu-Si interdiffusion during graphene synthesis and evaluated the use of metal and insulating diffusion barriers as a means of prevention at the Cu/SiO_2 interface.[107] Diffusion barriers (W, Cr, Ni, Al_2O_3, HfO_2, SiN_x) have been demonstrated to reduce interfacial diffusion, but often the Cu/Si interdiffusion was not

completely suppressed. To solve this, instead of using a similar process to grow on freestanding foils, the pre-growth annealing of the foil at a lower temperature (typically 700 °C) was carried out to achieve Cu grain growth; this also minimized the copper evaporation occurring at high temperature. Moreover, excessive exposure to high temperatures can result in the formation of voids in the copper film and decomposition of the film into islands.

Another reason for using thin films, mostly in the case of Ni and other metals with high solubility, was that the large amount of carbon sources absorbed on nickel foils usually formed thick graphite crystals rather than graphene films.[66,108] To solve this problem, very thin layers of nickel (thickness down to 300 nm) have been deposited on SiO_2/Si substrates using electron-beam evaporators. It was demonstrated that very thin films and rapid cooling proved critical in suppressing the formation of multiple layers.

3.2.3.2. Macro-roughness and morphology

It has often been found that the topography of the surface strongly affects the uniformity of grown graphene. Also it has been widely discussed that the purity of the film determines the number of layers, mainly under low pressure conditions.[30] Luo et al.[109] showed that the use of a very flat, electro-polished Cu catalyst surface and extremely low methane concentration enables the growth of a very uniform graphene film. Boundary structures on the standard Cu foil led to thickness variations in the graphene film. Raman measurements of the graphene film regions that replicate the Cu grain boundary regions revealed carbon atoms in disordered sp^3-bonded networks in these areas. The correlation of graphene thickness variation with the topography of the catalytic Cu foil motivated the idea that smoothing the Cu through polishing would lead to more uniform and better quality graphene. Moreover, first principles calculations indicated that, in contrast to graphene growth on other metals, Cu-catalyzed graphene nucleation was particularly favored at surface irregularities (i.e., metal step edges and other defects) but also occurs over the flat regions.[110] Therefore, nucleation was also found to proceed readily on the crystal plane and to be favored at high partial pressures.

3.2.3.3. Micro-roughness, boundaries, step edges

Theoretical works show that carbon binds more strongly at the step edges than on the terraces for transition metals such as Ni, Co, Ru, and Rh.[111] Even with full coverage along the step edge, carbon still binds most favorably to the step sites.[112–114] Metal atomic step edges were also demonstrated to be important for graphene island nucleation in the case of Cu, but not unique and in some cases not the most desired.

Regarding this, Wofford et al.,[29] showed that a minimum temperature of ~790 °C is sufficiently high to induce significant motion of Cu steps in LPCVD due to sublimation on Cu (100) foils. Real-time observations during synthesis demonstrated, at high temperatures above 960 °C, that the surface of each Cu grain consists of a propagating array of monolayer-height steps before growth. Subsequently, when a segment of a Cu step edge collides with a growing graphene island, it decelerates and incoming step edges become bunched under the graphene. As a consequence, incoming steps wrap around under the interior of the four-lobed graphene island. This process creates four-lobed Cu hillocks draped by graphene. Indeed, at very high temperatures, surface roughening can be so dramatic that individual hillocks can be easily visible with an optical microscope. While single Cu step edges was not observed to have a perceptible effect on the growth, large bunches have been observed to distort island evolution, to induce rotational disorder by altering growth trajectories, and to decrease the graphene quality.

In the case of graphene islands grown on Cu(111) under UHV conditions, it was also observed that Cu(111) step bunches led to rotational disorder in two ways.[115] First, they can cause islands to be nucleated with different in-plane orientations. Second, step bunches can generate new rotational boundaries as islands expand. Change of island orientation was observed when crossing a step bunch. Thus, fewer step bunches led to fewer rotational boundaries, consistent with the work of Zhao et al.[94] These high-angle rotational boundaries could be minimized using higher growth temperatures in this Cu(111) case.

The tendency to introduce rotational boundaries during growth differentiates Cu(111) and Cu(100) from other surfaces. For example, graphene sheets have been observed to grow without changing orientation across boundaries between rotationally misoriented Ru(0001) grains[116] and even across different facets of Ni grains. It is worthy of mention that temperature and pressure dependence of these processes have to be taken into account. As discussed below, compact hexagonal shapes have been observed in high-pressure CVD by several groups. The carrier and carbon-source gases in CVD suppress Cu evaporation, so that a higher temperature can be employed compared to that used with UHV growth. At high temperatures in UHV experiments, the surface morphology is evolving quickly due to sublimation, causing large step bunches to collect at graphene edges. Rearranging these step bunches is likely to be difficult, impeding the processes that lead to hexagonal shapes. Therefore, pressure and temperature seem to have a critical role in evaporation and propagation of metal atomic steps.

3.2.3.4. Other defects and impurities

It was observed that graphene initially nucleates on the Cu surface impurities, imperfections, step edges, and grain boundaries. Therefore, reducing the density of nucleation sites can effectively increase the graphene domain size.[65] It

was also observed that the type of nucleation site can affect whether the graphene island was single crystal or not; the latter result gives rise to a mean grain number much smaller than the nucleation density.[29] Polycrystals are preferentially formed on defective nucleation sites whereas single crystals do form preferentially at the less defective regions. On Cu(111), single-crystal graphene firstly nucleated inhomogeneously at defects such as steps, step bunches, and impurities,[115] but changing to proper synthesis conditions can lead to secondary single-crystal nucleation, more difficult to achieve because of the more difficult nucleation on less defective regions. The metal purity was considered as a meaningful aspect to yield higher quality graphene. It has been shown that higher purity copper foils (99.999%) yield higher quality graphene, with room-temperature mobility closer to those reported for exfoliated graphene.[117] Kalbac et al.[28] suggested that the graphene growth begins by the formation of a multilayer cluster due to complex defects or polycrystalline impurities. This seed was observed to increase its size but the growth speed of a particular layer depends on its proximity to the copper surface.

Liu et al.,[30] found that the purity of the Cu film clearly determined the number of synthesized graphene layers under low pressure conditions. Multilayer graphene was observed to nucleate from the impurity clusters and merge into a 1–2 layer graphene film away from the nucleation centers.

The above discussion reveals that it is crucial to reduce the number of imperfections, roughness, and impurities, and make the surface as uniform as possible to obtain high-uniformity graphene on Cu. It is clear that the roughness and imperfections not only enhance graphene nucleation initially, but also defective graphene later. It is also possible that the impurity atoms in the bulk diffuse to the Cu surface during annealing. These surface impurities dramatically enhance the catalytic capability of Cu, resulting in a high concentration of carbon atoms that are decomposed from precursors. Hence, it can be concluded that the purity of the Cu surface plays a critical role in determining the number of graphene layers.

3.2.4. Seeded Growth and Controlled Nucleation

Recently, new approaches dealing with pre-patterned graphene seeds have been investigated. Substrate-surface seeding is a common surface pretreatment method used to modify and control the surface nucleation density and the growth rate of diamond films.[118] In the case of diamond, powder or particles littered on the substrate surface have been used as the predominant nucleation sites, and the material was grown gradually owing to the C adatom concentration.

In the case of graphene on Cu, these new experiments have been performed in different ways, either using seeds of pre-patterned multilayer graphene flakes or controlling

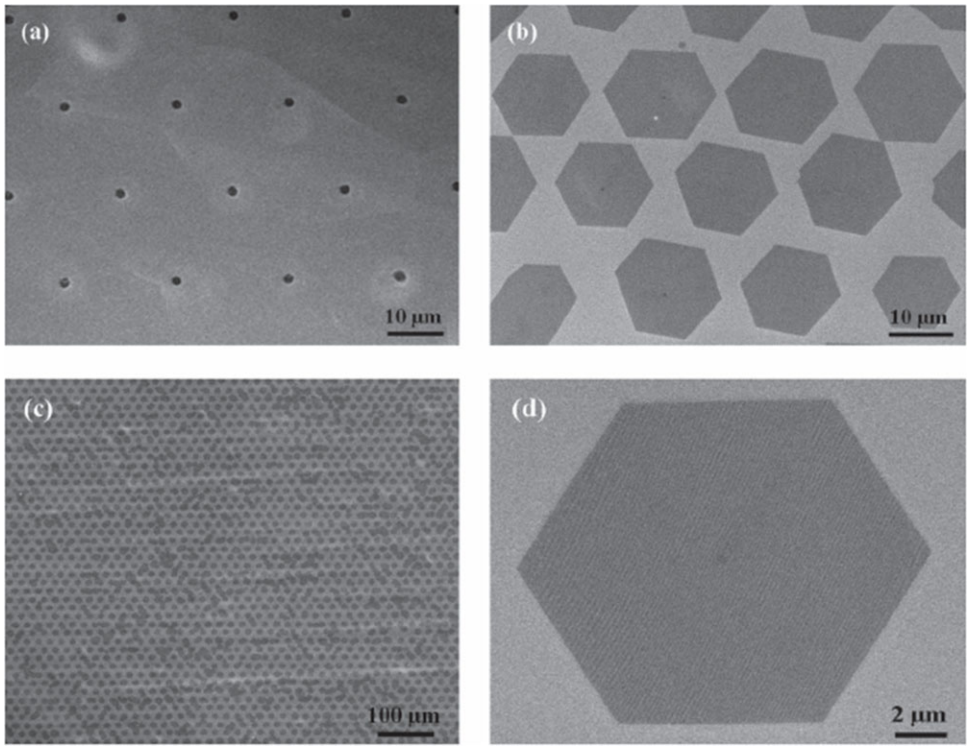

Fig. 7. SEM images of a) patterned PMMA dots; b,c) arrays of graphene grains after the CVD process at high and low magnifications, respectively; d) enlarged individual graphene grain. All images were obtained on Cu foils. Reproduced with permission [120]. Copyright 2012 Wiley-VCH Verlag GmbH & Co.

nucleation by locally providing a high concentration of carbon. In the former method[119] however, an extra CVD process was firstly required to obtain a continuous multilayer graphene film on Cu used for the following lithographic patterning of the growth seeds (multilayer graphene). In the latter method[120] (Fig. 7), PMMA was used as the carbon source during the APCVD process for enhancing local nucleation. This latter method demonstrated controlled graphene nucleation and synthesis of single-crystal graphene arrays, and offered a promising route to fabricate graphene-based devices free of grain boundaries and with more reliable performance. Occasionally, polycrystalline islands or few-layer domains, nucleated and grown from one single such nucleus, have also been observed. Also performed were some experiments with highly oriented pyrolytic graphite (HOPG) flakes as seeds transferred to the Cu foil surface, simply by pressing against the patterned HOPG. After the CVD synthesis, a preferential nucleation of graphene on HOPG sites was also observed. Due to the roughness and flexibility of the surfaces of those thin Cu foils, however, transferred graphite flakes differ significantly in size, thickness, and shape, affecting graphene growth. In addition, it was nearly impossible to fabricate well-defined arrays by the pressing method.

This seeded growth could be a very interesting alternative for high-quality and performance graphene layers with applications in several fields. Nevertheless, very high complex processes with important economic implications are involved.

3.3. Thermodynamic and Kinetic Parameters

Pressure and temperature have been revealed as key factors during graphene growth. Other dynamic factors, such as gas flow and gas residence time inside the processing chamber, also play important roles that will be reviewed in this section. We will also refer to other important aspects of the synthesis, such as plasma-assisted deposition and different time profiles during all the steps of the graphene deposition.

3.3.1. Pressure

Vacuum level prior to synthesis should be minimized to the limit in order to get high-purity layers. The lower the base pressure of the reactor, the lower the density of impurities and residual oxygen. Working in LPCVD, vacuum levels of a few mTorr have been commonly used. On the other hand, recipes with diluents (H_2) of the precursor gases have been proposed for reducing residual oxygen during the annealing and growing stages of the synthesis.

Up to now, a lot of experimental work has been published covering an extensive pressure range; HV (high vacuum, 10^{-4}–10^{-6} Torr), LP (low pressure 0.1–1 Torr), and AP (atmospheric pressure). It has been possible to grow graphene with acceptable quality in all ranges, but great differences in graphene domain size and morphology have been observed. In LPCVD, flower-like four- to six-lobed structures have been commonly grown.[6,59] In contrast, in APCVD, hexagonal structures of graphene have been synthesized.[120,121] Concerning the domain size, both cases offer graphene flakes near millimeter size, and continuous monolayer films when using Cu as a catalyst. Bhaviripudi et al.[121] studied, under the same experimental set-up, the role of the total pressure on Cu. The results revealed that, even though the thermodynamics of the system remains the same, whether the process was performed under AP, LP, or UHV conditions, the kinetics of the growth phenomenon were different. Although in LPCVD monolayer graphene was grown (up to 95% monolayer coverage), in the case of APCVD growth, results varied from a monolayer at lower (parts per million) methane concentration to multilayer domains with a monolayer graphene background at higher (5–10% by volume) methane concentration. This seems to indicate that either the growth was not self-limiting under higher methane concentration, or only partial coverage was achieved. This lack of control over the number of layers and the different domain shapes promoted further investigations performed to determine the detailed growth mechanism.

The more exciting difference between LP and AP may be the morphology and shape of the graphene domains, and was extensively studied in real-time LPCVD experiments.[29,115] In the case of APCVD, the tendency for the graphene grown into AB Bernal few-layer hexagonal stacks was also studied.[122] It was discussed that the growth of the top graphene layers with no contact with the copper surface could be due to the high local supersaturation of carbon at high methane flow rates with an excess of precursor supply. Higher precursor supersaturation should lead to considerably faster graphene growth, however low graphene coverage rate of $0.2\,\mu m^2\,min^{-1}$ was monitored, whereas considerably higher rates of up to $100\,\mu m^2\,min^{-1}$ have been observed for LP growth by Li et al.[31] It could be hypothesized that the lower growth rate could be due to lower lateral diffusion rate of species that favor multilayered graphene instead of monolayer fast growth.

To better support the discussion of the formation of multilayer graphene at an early stage and the limited further growth of the top layers, Wu et al.[123] developed a two-step APCVD process with a similar strategy to Li et al.[31] The result was consistent with the point that, once a continuous graphene film formed on the catalytic Cu surface, growth of an extra graphene layer was inhibited because of the absence of Cu to catalytically decompose the carbon precursor gas.[27]

Another significant factor related to the experimental pressure is the sublimation/evaporation during the process due to the vapor pressure (V_p). The V_p of the substrate was demonstrated to have a strong influence on the growth rate and orientation of the graphene grains.[29,79] V_p of Cu and Ni

are 6×10^{-5} and 1×10^{-7} Torr, respectively. For the Cu(111) surface, this represents a loss of four monolayers (ML) of Cu per second from the surface at 1000 °C under UHV conditions, whereas the sublimation rate from a Ni(111) surface is approximately 7×10^{-3} ML s^{-1}. For graphene growth on Cu substrates under a LP regime, the pressure of the source gas is typically in the mTorr range, which should slow the sublimation rate of Cu from the surface. Even so, sublimation of metal during growth was reported due to the high temperature commonly used, close to the melting point of the copper (1084 °C), and even more under a LP regime. Significant amount of the copper evaporates and deposits at the edges of the fused silica tube used in the CVD, however once graphene growth was initiated, the graphene-covered regions of the surface have been observed to suppress sublimation.

Sublimation of the metal catalyst during the growth was used to deposit monolayer graphene, although this parameter should be precisely controlled.[91,124] Defective films have been grown using sacrificial copper films. One cause of the defective film could be that the grown graphene can break under stress due to the Cu morphology change during its evaporation.

It is worth mentioning that Liu et al.[30] noticed that decreasing the annealing pressure (from 80 to 20 mbar) could have a positive effect on the quality and uniformity of graphene. It was observed that the surface of Cu became smoother due to the increasing sublimation of Cu at lower pressure. Low pressure during annealing could greatly enhance the uniformity of the Cu surface and decrease the number of the sharp structures, thereby making the Cu surface smoother. It has already been demonstrated, however, that in the growing stage[29] Cu sublimation should be avoided due to roughening of the Cu surface and, subsequently, the conformal graphene film.

3.3.1.1. Partial pressure of precursor gases and hydrogen

Recent studies on graphene growth optimization indicated that hydrocarbon pressure is one of the major factors affecting graphene growth.[31,123] In most of the experiments a minimum partial pressure of hydrocarbon is required for graphene to cover the Cu surface during growth. The pressure of the hydrocarbon determines the concentration of the carbon species on the Cu surface during graphene growth. Therefore, a controlled and relatively low precursor (CH_x) partial pressure is highly recommended in all pressure ranges.[109,121] This was also demonstrated by Li et al.[30] during the synthesis of high quality graphene working under very low total pressure (mTorr range) with almost only carbon precursors and a low quantity of H_2.

Zhang et al.[125] investigated the correlation between the grain morphology and the total pressure and methane-to-hydrogen ratio in LPCVD processes. With a methane-to-hydrogen ratio of 1:12.5 and under different total pressures, the graphene grains changed from irregular small flakes (80 mTorr) to mostly four-lobe grains (100 mTorr), and finally to mostly six-lobe flowers (150 and 200 mTorr). When increasing the total pressure to 300 mTorr, the six-lobe graphene flowers turned to irregular shape. Interestingly, similar results have been obtained when keeping the total pressure at 150 mTorr, and gradually increasing the methane-to-hydrogen ratio from 1:30 to 1:2. All these observations indicated that increasing the total pressure of the CVD system had a similar effect on the morphology of graphene grains as increasing the methane-to-hydrogen ratio.

The role of hydrogen partial pressure has already been commented on (see Sec. 3.1). Gao et al.[71] observed that the graphene edges became regular and straighter, because edges with a low stability had been selectively etched away by an active atomic H when the CH_4/H_2 ratio was low. Wang et al.[126] also studied the role of hydrogen. They observed that only when the CH_4 supply was shut off and the sample was cooled, after the growth stage, in a high concentration H_2 atmosphere (300 sccm Ar and 40 sccm H_2), did the graphene domains appear to be etched into rectangular openings. In accordance with the copper-catalyzed etching mechanism recently proposed, Zhang et al. showed that low concentration H_2 could reduce the etch rate considerably and result in no significant etching damage.[127]

This section has revealed that the pressure regime is crucial in high-quality graphene synthesis. It seems that more regular graphene domains are synthesized by APCVD. LPCVD regimes enhance the evaporation of the catalyst and produce etched domains, but more precise control of the number of layers is achieved. The role of hydrogen remains an open question to be resolved, although etching effects have been demonstrated. The partial pressure of the precursor gases has been revealed as crucial and dependent upon reactor set-up although some relationship between this partial pressure and the total pressure of the system was detected.

3.3.2. Temperature

One important effect, widely detected in tubular reactors, is the temperature gradient along the radial direction inside the reactor. This can result in inhomogeneous growth of the graphene. To solve this, two quartz tubes, one suspended inside the other, have been used in large-area synthesis experiments, the small tube being wrapped with a metal foil.[7]

3.3.2.1. Heating treatment of the catalyst

In catalysis, an enhanced dissociation of carbon precursors at high temperature and also surface smoothing via metal grain growth (this is a fundamental step in graphene synthesis over metal foils) has been demonstrated. Depending on the catalytic activity of the metal, the process temperatures can vary between 800 and 1100 °C. Ni has been intensively studied because the phase diagram of Ni and C

reveals that, at high temperature, a solid solution is formed (above 800 °C) and that the metastable formation of Ni_3C phase promotes the precipitation of carbon out of Ni. Co and Fe show also carbon solubility at 850–1000 °C, although graphite precipitation from Fe can be obtained only under very specific conditions. Working with Cu and Ni it is common to use temperatures in the range 900–1050 °C. It has been demonstrated that high T (>1035 °C) yields a low density of graphene nuclei when growing and, as a consequence, large domain size. But the problems with high temperatures were that more metal was observed to evaporate, depending on pressure conditions, and that the roughness of the surface was promoted.

A "hot-wall" reactor, consisting of a quartz tube located inside a furnace, is the configuration most used in graphene synthesis.[7,129,130] On the other hand it is believed that, in this type of reactor, thermal gas activation and dissociation in the gas phase may be considered as not particularly noticeable. Therefore, if the reaction is surface-limited (heterogeneous reaction) there is no need to heat the gas to this high temperature before it reaches the surface. There is another possibility, the "cold-wall" type of apparatus where only the substrate is heated, and in less time. The cold-wall reduces the gas-phase reactions completely, resulting in no particulate contamination. Synthesis of high-quality graphene films on Ni foils, using a cold-wall reactor with a rapid thermal processing (RTP) heater, has been reported.[128] RTP provided fast heating and cooling rates, and temperature control. The reported results differed from previous observations in the growth of graphene on Ni substrates by CVD due to the rapid process, even enabling new discussions about growth kinetics. These results suggested that, in the case of Ni, two different growth mechanisms could exist. While a portion of carbon atoms may be dissolved into the nickel film, many carbon atoms also migrate to the nickel surface and bond with each other to form graphene. Therefore, this could explain the graphene synthesis in a very short growth time (30 s); this direct growth-surface migration mechanism may play a larger role than the precipitation mechanism. To verify the direct growth mechanism of the CVD process, very short growth time (10 s) and various H_2 gas flow rates during the growth stage have been investigated. The defect density decreased with a decrease in the H_2 flow rate. It could be postulated that hydrogen is not necessary to synthesize high-quality graphene by a RTP direct-growth mechanism using a Ni catalyst, consistent with the previously observed in the case of CVD growth of graphene on Cu foils.[131]

The concept of the cold-wall reactor may be extended to other approaches recently published. As an example, high-quality graphene grown by selective Joule heating at 950 °C on copper foils with extended areas, was demonstrated by Kobayashi et al.[8] The direct transfer of high-quality as-grown graphene was also demonstrated.

Geng et al.[132] demonstrated that the use of liquid Cu ($T > 1084$ °C, Cu melting point) can be particularly effective for controlling the nucleation process in graphene APCVD systems. It was observed that the grain boundaries have been eliminated, and the results showed the production of uniform, self-aligned, large-sized, single-domain, hexagonal graphene flakes (HGF) and continuous monolayer films (Fig. 8). This new route involved the formation of a liquid Cu phase on quartz and W substrates at growth temperature above the Cu melting point. The evolution from well-separated HGFs, to closely packed structures and to continuous film was documented. Typically, HGFs well dispersed on the surface and self-assembled have been observed. The liquid Cu surface could be involved in the translation or rotation of HGFs, while a minimization of the surface energy may be responsible for the alignment. The average size of individual HGFs determined by both nucleation density and growth rate was about 20–30 μm. Increasing the growth temperature led to HGFs with average sizes of approximately 50 μm; and lowering the CH_4 flow rate led to a size of approximately 120 μm. The average growth rate of HGFs was estimated to be 10–50 μm min^{-1} on flat Cu/W, which is much higher than the rate of 0.1–0.2 μm min^{-1} observed for the case of HGFs grown on a Cu solid surface.[133]

3.3.2.2. Low-temperature synthesis (plasma-assisted processes)

Low-temperature processes for graphene synthesis are highly recommended for industrial applications. There is still a need to develop a reliable and reproducible method for the low-temperature synthesis of high-quality graphene for the full exploitation of graphene properties and application potentials. One game-changing breakthrough would be the development of graphene growth on arbitrary surfaces at low temperatures (for example, by means of plasma-assisted deposition) with a minimal number of defects.[134] Therefore plasma-assisted deposition could be a fundamental player in the future development of graphene.

Different works using surface wave plasma (SWP)-CVD and remote PACVD exhibited a capacity to synthesis graphene at lower temperatures and over substrates other than those used in standard processes (Al foil).[135] In the former method no monolayer graphene was deposited, but in the latter method FLG was synthesized at a relatively higher temperature of 650 °C. In another approach by Kim et al.,[136] graphene films have been synthesized on polycrystalline nickel foil using a cold-wall, microwave plasma-assisted (MP) CVD system with a heating stage. A substrate temperature of 450 to 750 °C and a total pressure of 20 Torr have been used with various mixing ratios of H_2 and CH_4. The dependence of monolayer graphene synthesis on temperature was investigated, and it was clearly shown that the higher the temperature the higher quality graphene could be grown.

Teresawa et al.[137] investigated multilayer graphene grown on Cu foils by radio-frequency plasma-enhanced

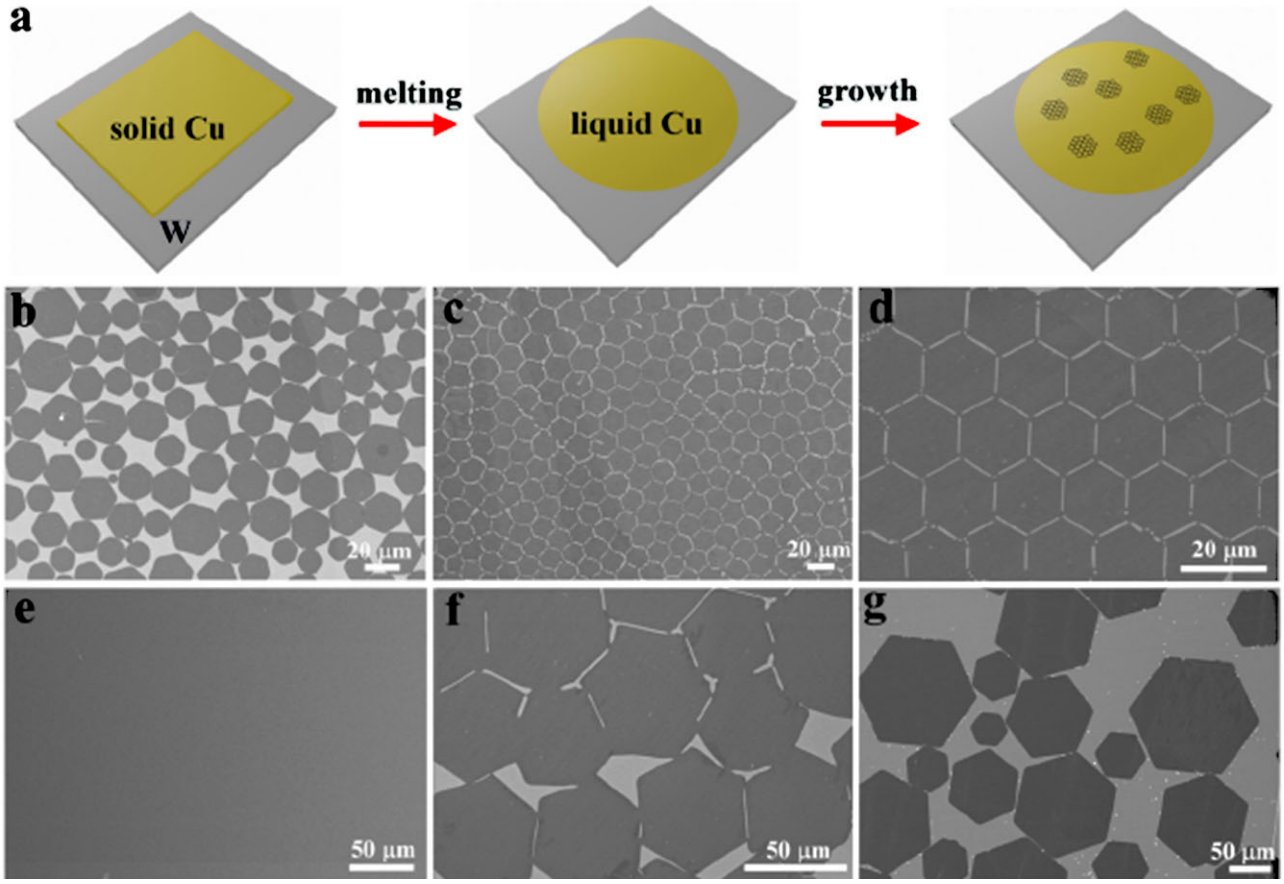

Fig. 8. The growth of HGFs on flat liquid Cu surfaces on W substrates. a) Scheme showing the CVD process for the synthesis of HGFs on liquid Cu surface. b) SEM image showing partially covered and well-dispersed HGFs using 6 sccm CH_4/300 sccm H_2 at 1.120 °C for 30 min. c) SEM image showing a compact assembly of HGFs in which the dark and bright parts represent HGFs and the Cu surface, respectively. d) SEM image of a near-perfect 2D lattice composed of similar-sized HGFs. e) SEM image of the sample for 2 h growth showing the continuous graphene film with uniform contrast. f,g) SEM images of large-sized HGFs showing that the average sizes are approximately 50 μm and approximately 120 μm using 1.140 °C and 1.160 °C, respectively. Experimental conditions for (c) and (d) are the same, using 6 sccm CH_4/300 sccm H_2 at 1.120 °C for 38 min. Reproduced with permission [132]. Copyright 2012, National Academy of Sciences, USA.

(RF-PE) CVD. The growth of graphene was investigated under various conditions, such as changing the plasma power, gas pressures, and the substrate temperature (from 500 °C to 900 °C). At high substrate temperatures, the growth of the first layer of graphene was affected by the catalytic action of Cu, while the growth, at low temperature, of multilayer graphene was dominated mostly by radicals generated in the plasma. Outstanding differences in the grain size, number of layers, and growth rates on FLG at 500 and 900 °C have been observed. It was also observed that the grain size of graphene decreases with the thickness. The growth rate of the subsequent layers in multilayer graphene was measured to be approximately five times slower than that of the first layer. In thermal CVD, the difference in the growth rate between the first layer and the second layer was more than tenfold.[27] This more rapid growth, compared with thermal CVD, is one of the features in PECVD. In contrast to thermal CVD, an activated carbon fragment, such as the C2 radical, is formed in PECVD and graphene growth occurs even at 500 °C.

Rapid synthesis RF-PECVD was revealed as a very powerful technique for the synthesis of large-scale graphene at relatively low temperature and in a short time.[138] Large-area single- or multilayer graphene of high quality was synthesized on Ni films deposited on a thermally oxidized Si, at a relatively low temperature (650 °C). In the deposition process, a trace amount of CH_4 was introduced into the PECVD chamber, and only a short deposition time (30–60 s) was used. Single- or multilayer graphene was obtained due to carbon atoms from the discharge diffusing into the Ni film and then segregating out at its surface. Increasing number of graphene layers were obtained with longer deposition times using larger CH_4 flows at a cooling rate of about 10 °C s^{-1}. Kalita et al.[139] reported the direct synthesis of nano-graphene films (very small domain size) on silicon (n-Si) and glass (SiO_2) substrates by microwave-assisted surface wave-plasma (MW-SWP) CVD at 400–560 °C. The technique is a rapid growth process (70–120 s) and the film can be deposited on various substrates. The directly grown deposit consisted of triangular-shaped nano-graphene domains with

lengths of 80–100 nm that interconnect to form a continuous film. For the deposition process, a gas mixture of C_2H_2 and Ar under a pressure of 45 Pa was used. Kumar et al.[140] reported a unique process for rapid synthesis (100 s duration) of FLG films on Cu foil by microwave plasma (MP) CVD. The process can produce films of controllable quality from amorphous to highly crystalline by adjusting plasma conditions during growth, and with no supplemental substrate heating (plasma-metal coupling for rapid heating of the foil). The hydrogen plasma was also used to remove the native oxide layer enabling graphene growth on metal Cu. It was suggested that the same process could be used for rapid synthesis of primarily single-layer graphene.

Great advances are being published in this area of graphene synthesis. Monolayer high-quality graphene on metal has been synthesized at lower temperatures. Synthesis of small-domain graphene on dielectric substrates has also been published. Therefore, low temperature processes for graphene synthesis by means of plasma-assisted deposition are being developed. This will be an extensive area of research in the near future, with the intention to synthesize a controllable number of graphene layers on arbitrary substrates with a reliable and reproducible method.

3.3.3. Gas Flow Rate and Residence Time

The gas flow regime has been revealed as an important factor to be taken into account during graphene synthesis. It has also been observed that the density of graphene nuclei decreased as T increased or as methane flow (J_{Me}) and methane partial pressure (P_{Me}) decreased. Therefore, high T and low J_{Me} and P_{Me} were found to yield a low density of graphene nuclei and thus a large domain size.[31] Various vapor-trapping methods have been reported. Li et al.[59] demonstrated the CVD growth of graphene single crystals up to 0.5 mm in size in a quasi-static flow regime (vapor-trapping method), using a copper enclosure in LPCVD. Subsequent experiments in quasi-static flow achieved the growth of large-grain, single-crystalline, six-lobe graphene flowers with grain size up to 100 μm. Scanning electron microscope (SEM) images of these six-lobe graphene flowers grown on the bottom side of a Cu foil placed inside a vapor-trapping tube were shown.[125] Interestingly, the graphene grown on a Cu foil placed outside the small vapor-trapping tube did not show any "flower" shape, but continuous graphene film with slight etching. This result indicated that the vapor-trapping tube changed the local environment inside the tube, especially in reducing the carbon supply and creating a quasi-static reactant gas distribution that resulted in large flower-shaped graphene grains.

Following this line of experimentation, using Fe foils while keeping the other parameters unchanged, when the methane flow rate decreased (from 300 sccm to 180 sccm), bilayer graphene instead of multilayer was obtained, likely due to the smaller amount of carbon dissolved and segregated from the catalyst.[76]

3.3.4. Heating/Cooling Treatments and Process in Steps

3.3.4.1. Annealing time

Reducing the nucleation density was a feasible route to prepare large-size, single-crystal graphene domains.[59] The presence of impurities and defects on the surface of a substrate was shown to affect the nucleation behavior considerably. Regarding the importance of surface defects, Gao et al.[143] demonstrated that the graphene nucleation rate near a step edge may be 10^4–10^7 times greater than that on a terrace due to a significantly lower nucleation barrier. As known, high-temperature treatments of the substrate revealed to be helpful for the reduction of volatile impurities, contaminants, and defects on a copper surface, thus leading to the hindering of graphene nucleation. Very longtime annealing (3 h) was also used by Wang et al.[126] to reduce the nucleation density on copper foils resulting in large hexagonal domains about 0.4 mm × 0.4 mm.

The effects of total annealing time and temperature on the orientation and size of grains within Cu foils and CuNi alloy foils were also studied.[79] As discussed above, alloying metals is often performed in order to control the number of graphene layers. The annealing process could be summarized in two stages. During the grain growth, the first step is to incorporate and order atoms from the disordered regions, resulting in some ordered regions. The second step is the growth of large grains at the expense of smaller ones. As the temperature increases to a value close to the melting point of the metal, the diffusion coefficient of the atoms within the foil becomes very large (atomic diffusion is a thermally activated process), resulting in the growth of grains with macroscopic dimensions. The obtained results showed typical lateral dimensions ranging from a few millimeters up to approximately a centimeter for Cu foils annealed at 1030 °C for 35 min, and from tens of micrometers up to a few hundred micrometers for the 90/10 CuNi foils annealed at 1050 °C for times ranging from 45 to 90 min. The smaller grains within the CuNi foils were attributed to the higher melting point of the CuNi alloy. Then, at these temperatures, a higher density of grain borders and subsequent defects on as-grown graphene can possibly occur on alloys.

Concerning the effect of H_2 during the annealing treatment, it is believed that H_2 can eliminate certain impurities such as sulfur (S) and phosphorus (P) that may cause local variations in the carbon dissolvability in the metal substrates.[144] Therefore, it seems clear that long annealing times under low pressure of reducing gases, combined with high temperature, yielded low nucleation density and subsequently large domains. This route is highly desirable in high-quality graphene synthesis.

3.3.5. Growing step profile

In the pioneering work of Li et al.,[31] a two-step process in LPCVD, varying the partial pressure of methane for large-domain graphene synthesis, has been proposed. For a given temperature (usually 1035 °C) nuclei were formed in a first

step under low methane partial pressure and flow. In a second step, the partial pressure of the methane was increased to promote full surface coverage. It is important to note that, for a given temperature and partial pressure, once the nuclei density was set, no significant new graphene nuclei were detected. According to this work, other groups[126] employed the same strategy during the growth process. It was clearly observed that diminishing the CH_4 concentration leads to a reduction of graphene nucleation. Wu et al.[123] also developed a two-step APCVD process with a similar strategy to Li et al.[31] Graphene growth was carried out at 1050 °C, introducing various amounts of CH_4. Initially, with low CH_4 concentration (5 ppm), low nucleation density was guaranteed. After 20 min, the growth was continued by increasing CH_4 concentration (55 ppm), without changing any other conditions, to get complete graphene coverage.

Finally, other studies[145] have been developed including a two-step, APCVD process, combining a surface-catalyzed process with segregation from bulk, to grow bilayer graphene. Carbon atoms were first dissolved in the quasi-melting Cu metal, and then segregated on the Cu surface to form nucleation centers.

3.3.5.1. Cooling ramp

The role of the temperature gradient during the cooling step after the synthesis process was demonstrated to be a critical factor, especially when working with a high carbon solubility catalyst (e.g., Ni).[25] Considering Fick's laws of diffusion, the area of FLG should dramatically increase in samples subjected to a slow cooling process. Therefore, high cooling rates, among other strategies, were commonly used to avoid (or make more difficult) carbon segregation in high-solubility metals, providing success in the growth of high-quality FLG. As commented on above, high-quality monolayer and bilayer graphene were synthesized by using rapid processes and high cooling rates. Even when thin layers of nickel are deposited on SiO_2/Si substrates to avoid the large amount of carbon diffusing into nickel foils, a fast cooling rate is critical in suppressing the formation of multiple layers.[26] Unexpected results were also published, where the contrary was also observed in graphene samples fabricated using both slow and fast cooling rates (0.3 and 3 °C s^{-1}).[129] A possible explanation could be that, under particular experimental conditions, the surface-mediated mechanism (as for the Cu case) plays a larger role in final film formation than the precipitation mechanism. As is likely, both mechanisms will occur simultaneously during graphene growth. It was pointed out that the growth mechanism proposed for Cu systems[6] may, in some cases, be applicable to the Ni system, if the synthesis conditions are suitable to control to the minimum the bulk-diffusion of the carbon into the metal, and the catalysis of the decomposition of the precursor gas is effectively achieved.

Interestingly, it was also found that the cooling rate may control the segregation behavior, strongly affecting the thickness and quality of the graphene deposit.[141] Because the concentration of carbon decreases exponentially from the surface into the bulk, an extremely fast cooling can have a quenching effect, reducing the rate of carbon migration to the surface. Otherwise, extremely slow cooling rates can result in carbon with enough time to diffuse into the bulk, subsequently avoiding carbon segregating at the surface, strongly affecting the crystallinity. These results suggest that several layers of high-quality graphene can be synthesized on a Ni surface with optimized, medium cooling rates. It was also observed that the same gas mixture should be used during the cool-down to prevent the loss of carbon from the graphene over-layer (e.g., formation of CO and CO_2), which can occur at temperatures higher than 300 °C.[79]

Published results of graphene synthesis on Cu have also shown that high vacuum, depletion of hydrogen, and slower cooling rate (18 °C min^{-1}) compared to previous single-layer graphene synthesis, can produce CVD growth of bilayer graphene.[142] It was also found that in APCVD on Cu, the cooling rate can significantly affect the number of layers in the graphene domains. High-quality monolayer graphene domains were only obtained with low cooling rates, while high cooling rates result in multilayer graphene domains with more defects.[126]

4. Scalability and Industrialization

One favorable aspect of graphene synthesis by CVD is the ability to maximize the scale without losing the homogeneity of large-area films, as published by Bae et al.[7] An 8" wide, double tubular, quartz reactor was used in the CVD system, allowing a monolayer graphene film to be synthesized on a roll of copper foil with dimensions as large as 30" in the diagonal direction. Excellent optical properties were measured on these films, after layer-by-layer transfer to dielectric substrates, achieving bilayer, tri-layer, and four-layer graphene.

A new and innovative approach to the CVD synthesis of ultra large-area graphene based on selective Joule heating was presented by Kobayashi et al.[8] A continuous roll-to-roll and transfer process using copper foil and photo-curable epoxy resin allowed the fabrication of graphene transparent conductive film, up to 100 m long, with sheet resistance as low as 150 Ω per sq. The graphene was grown at temperatures around 950 °C, applying a constant direct current of $J = 82\,A\,mm^{-2}$ to the copper foil suspended between two current-feeding electrodes. To the best of our knowledge, this is the largest graphene area synthesized and demonstrated by far.

Roll-to-roll MPCVD was also used for the continuous deposition of graphene films in industrial mass production.[146] A deposition area of 294 mm × 480 mm was demonstrated. FLG films, which consist of flakes with a nanometer size, were deposited onto a Cu foil, although it was expected that graphene films can be obtained on other substrates by optimizing the deposition conditions.

5. Bilayer Graphene

Bilayer AB (Bernal) stacked graphene became a very interesting option in electronic applications. The stacking order and coupling in FLG were demonstrated to affect the electrical properties of the material,[147] however a process of layer-by-layer transfer could not produce AB stacked graphene due to the random orientation between the transferred layers. On the other hand, by means of better control of the CVD process, bilayer graphene was grown directly on metal substrates.[55,142,148] Typically, bilayer graphene was grown by feeding the growth system at a higher rate of carbon or a lower rate of H_2, but the exact growth conditions vary from one system to another due to process differences.

Lee et al.[142] reported the first synthesis of wafer-scale bilayer graphene film over at least 2" × 2" area, limited only by the synthesis apparatus. The method was based on the growth by CVD of bilayer graphene on a copper thin film surface, and was characterized by the depletion of hydrogen, high vacuum, and, most importantly, a slower cooling rate compared to previous single-layer graphene synthesis. The optimal bilayer graphene film was grown at 1000 °C, with a growth pressure of 0.5 Torr, a CH_4 flow rate of 70 sccm, and a cooling rate of 18 °C min^{-1} (0.3 °C s^{-1}). Characterization results confirmed highly homogeneous bilayer graphene film, with only a very small fraction corresponding to possibly three layers. The authors speculated that the key parameter for bilayer growth was the slow cooling process in comparison with publications of bilayer growth on other substrates.

More recently, Bi et al.[145] developed a two-step, APCVD process, combining a surface-catalyzed process with segregation from bulk to grow bilayer graphene. The yield of the bilayer graphene was demonstrated to be over 90%. The Cu foil was first placed in a horizontal, quartz tube and heated to 1080 °C under H_2 flow, and the CH_4 flow was then introduced into the chamber at 1080 °C. The furnace was then switched off, and cooled to a certain temperature. Finally, the CH_4 flow was turned off and the Cu foil in the quartz tube was withdrawn for rapid cooling. The graphene domains were prepared varying only the growth time between 3 and 10 min. These graphene crystallites spontaneously act as templates to induce the carbon atoms to form hexagonal, bilayer graphene domains, size-tunable by controlling the growth conditions. A yield over 90% of the bilayer graphene, with defect-free domains 100 μm in size, was demonstrated.

6. Graphene Nano-walls, Nanoribbons, and Nano-meshes

6.1. Nano-walls

Various publications on the field of graphene nano-walls, nanosheets, and vertically synthesized graphene have appeared in recent years. One pioneering experiment, to the best of our knowledge, was reported by Wang et al.[153] By means of inductive, plasma-assisted deposition, vertical nano-walls were deposited, without a catalyst, on a variety of substrates. These carbon nanosheets had a high density of atomic-scale, vertical graphitic edges that are potential sites for electron field emission. Malesevic et al.[154] discussed the growth of these type of walls in their microwave plasma-assisted experiments. They proposed that freestanding FLG nucleates from upward curling crack edges. Internal stress due to temperature gradients, ion bombardment, and a mismatch between the lattice parameters of the substrate material and graphite are thought to be the main reasons for the formation of cracks. In other experiments, the discussion of the nucleation of the nano-walls includes the possibility that a glassy carbon film first graphitizes on the microwave plasma-heated surface, followed by the growth of carbon nano-walls.[140] From the gas phase point of view, microwave plasma deposition of carbon nano-walls could be governed by the formation of C2 radicals in the plasma when using medium-to- high temperatures and Ar diluted plasmas during synthesis.[155] A recent paper on the hetero-epitaxial nucleation and growth of graphene nano-walls on silicon substrates also a proposed growth mechanism based on the preferential etching of Si(100) planes and nano-walls nucleation on selected Si(111) nano-facets.[156]

6.2. Nanoribbons

Theoretical and experimental data suggest that, like bilayer graphene, a band gap could be opened in sub 10 nm width graphene nanoribbons (GNRs).[149] The first synthesis of GNRs was performed through mechanical exfoliation in solution. Carbon nanotubes (CNTs) were also proposed as precursors for higher yields.[150] In this context, few-layer nanoribbons were produced by unzipping multi-walled CNTs using a two-step technique that included oxidation and dispersion in an organic solution by sonication.[157] Another interesting approach was microscopy-based patterning, limited by the wavelength of light and high cost.

6.3. Nano-meshes

Other graphene nanostructures, including graphene nano-meshes (GNM), were proven to be effective for opening the band gap. An interesting approach in the case of graphene nano-mesh synthesis by means of self-assembled colloid spheres and a metal mask deposited to fill the space between them was proposed by Bai et al.[151] Wang et al.[152] also demonstrated that smooth-edged graphene nanostructures can be directly grown on patterned copper foil by means of nano-sphere lithography.

7. Other Concepts: Laser CVD and Rapid Synthesis

Although CVD can achieve the scalable growth of graphene using a roll-to-roll method, fabrication of graphene patterns can only be performed with the aid of expensive and time-consuming post-lithographic processes. Therefore, a convenient approach to achieve fast, scalable, and affordable production of graphene patterns for electronic applications is widely required. A recent overview of laser-assisted techniques developed for fabricating carbon nanostructures, including graphene, nanotubes, and nano-onions was presented by Zhou et al.[158] Rapid, single-step fabrication of graphene patterns was achieved using laser direct writing. Line-shaped graphene ribbons of controlled widths and lengths were precisely fabricated on a Ni foil without extra annealing and lithographic patterning procedures. The localized laser heating resulted in a rapid thermal process at the laser beam focal point. Surprisingly, the growth rate of graphene was 1000 times faster than a conventional CVD method. Graphene patterns could be fabricated at a high scan speed up to 200 $\mu m\,s^{-1}$, much faster than a traditional fabrication approach. Direct writing graphene patterns using the laser CVD method could expand the capability of CVD approaches in rapid and controllable fabrication of graphene for a wide range of applications. High quality of the as-grown graphene was demonstrated by Raman spectroscopy. The number of graphene layers could be strictly controlled by the scan speed of the laser beam. Micrometer-size nano-ribbons with limited width were also synthesized.

8. Summary and Outlook

An in-depth review of the synthesis of graphene by CVD techniques is presented, compiling the latest, more meaningful results obtained in numerous laboratories around the world. The preparation of graphene deposits necessarily requires following some definite steps, such as a slow enough supply of carbon species to the growing surface that allows surface diffusion of carbon atoms over the substrate. Various precursors (in solid, liquid, or gas form) may be used as the source of carbon atoms for the preparation of graphene. Among these, a mixture of hydrocarbon and hydrogen (and particularly methane/hydrogen) is most widely used.

Following these guidelines, it is worth noting the importance of the presence of a metal for catalyzing the decomposition of precursor molecules. In this way, it is possible to control the decomposition process that supplies carbon atoms. As shown, the deposition mechanism strongly depends on the characteristics of the specific metal used as substrate/catalyst. Among these characteristics, the catalyzing efficiency as well as the solubility of carbon into the metal bulk have to be highlighted. Therefore, for metals with high carbon solubility (Ni, Co, …), the main growth mechanism is the segregation and precipitation of carbon atoms located through the metal bulk immediately after the catalytic CVD process. For low carbon solubility metals (Cu), however, the deposition mechanism is mainly dominated by the metal surface, and the graphene is formed outwards from the surface. Hence, the metal used as substrate/catalyst determines the main mechanism for the graphene growth. Moreover, the characteristics of the metal surface, where the growth process takes place, is essential in determining the final number of layers in the graphene deposit. Therefore, the metal substrate has to be properly treated in order to chemically reduce the metal surface and modify its structure by controlling the crystal orientation, increasing the grain size, and therefore ensuring the metal surface becomes smoother.

Recently, some approaches to control the number of layers of the graphene deposit via metal alloys catalysis (involving Ni) have been performed. There have been some important advances in controlling the growth of FLG by varying the composition of the metal alloy catalyst, although the physical, optical, and electronic properties of the films still have to be improved. Also, it would be highly desirable to directly grow graphene layers on dielectric substrates. More experimental work should be performed in these areas for graphene to be competitive on practical applications.

Up to now, the best approach to control the monolayer growth has been performed on a very low solubility metal, as Cu, since it was quite difficult to control the growth of monolayer graphene via fast cooling processes on high solubility metals (Ni), however rapid synthesis could give an opportunity to these metals. From a theoretical point of view, as copper substrates are used, CH is the most favorable carbon species coming from methane decomposition. Subsequently, on the metal surface, the energetically favorable dimer formation from the CH species will occur. The dimer formation, as well as the diffusion of the dimer over the copper surface, are the dominant processes with respect to the back dissociation of dimers, and the migration of carbon atoms either over the surface or towards the metal bulk. Therefore, when graphene is grown on copper foils, the main growth mechanism includes dimers as intermediate species. Dealing with the synthesis of extremely high-quality, single-crystalline, and millimeter-size graphene domains on Cu foils, great progress has been achieved recently, and many groups reported the growth of millimeter-sized graphene domains under various pressure regimes. These reports confirmed the use of Cu foils as an effective catalyst and substrate material for single-crystal, monolayer, graphene growth.

Also, it is worth mentioning that, in Cu-catalyzed, CVD-produced graphene growth, the hexagonal lattice of Cu(111) favored the high quality of the as-grown graphene. Moreover, during the CVD hetero-epitaxial growth on Cu(111), the orientation of graphene nuclei became well controlled with domain boundaries atomically connected. Therefore, it could be advantageous to develop techniques

for producing foils with a preferential (111) surface texture. Also, it has been shown that, for obtaining high-uniformity graphene, it is crucial to minimize the number of imperfections, roughness, and impurities, making the surface as uniform as possible. It is clear that, initially, the roughness and imperfections on the growing surface enhance graphene nucleation, however, during subsequent growth stages, the formation of a huge amount of defects is evident and thus the final deposit contains too many structural defects. Lastly, during annealing, the impurity atoms are likely to diffuse towards the Cu surface, often enhancing the decomposition of the gas precursor.

Finally, pressure and temperature are also decisive parameters for the successful growth of CVD-produced FLG from hydrocarbon/hydrogen gas mixtures. Low-pressure regimes enhance the evaporation of the catalyst and etched domains, although the control of the number of layers seems to be more precise. It should be highlighted that the role of hydrogen remains an open question to be resolved, although etching effects were demonstrated. As expected, the partial pressure of precursor gases is shown to be crucial, and depends on each reactor set-up. Another significant remark is that long annealing periods of the metal substrate/catalyst under low pressure in a reducing gas combined with high temperature, leads to a low nucleation density and afterwards large domains, both facts highly desirable for high-quality graphene synthesis. High temperature during annealing and growth, low partial pressure of carbon precursor diluted in hydrogen at low flow rates, and long exposure times have been demonstrated to be crucial factors on the growth of single-crystalline, monolayer domains. Additionally, evaporative loss of Cu should be suppressed during low-pressure synthesis.

The future development of CVD synthesis of graphene should go along parallel paths to achieve different objectives depending on application. Direct synthesis at low temperature on the desired functional substrates, controlling the number of layers with suitable layer geometry, avoiding post growth layer transfer and etching processes (as gap opening is desired), is the ultimate goal of the graphene roadmap, however along each path a series of preliminary steps should be given. In this context, and mainly in large-area applications (optics and optoelectronics), prior to the direct growth, catalyst engineering could be an intensive area of research due to the importance of surface texture in the as-grown graphene. Large-area, millimeter domain-sized, monolayer graphene has, so far, only been demonstrated on metals. Metal alloys may play a significant role in high-quality multilayer growth. Control of thermodynamic and kinetic parameters for the synthesis is not likely a drawback in future, and many groups have already demonstrated that it can be well controlled, even using economic precursors. It should be taken into account that high temperatures are needed in all these cases. There must be a great effort in this aspect, and low-temperature processes for graphene synthesis are being developed by using plasma-assisted deposition. This will be an extensive area of research in the near future, with the intention to synthesize a controllable number of graphene layers with large domain size, either on metals or arbitrary substrates, with a reliable and reproducible method. It would be of great interest to perform more experimental work to avoid the high nucleation density that has been detected in plasma processes by many groups. The high density of nucleation prevents the increase in domain size that is desirable in large-area applications. On the other hand, this could be an opportunity in the other set of small-area electronic applications that might include photovoltaics, where small-size graphene domains, graphene nanoribbons, and nano-dots are suitable, and gap opening due to quantum confinement desirable. Indeed, nano-graphene dots with variable layer number and domain size from units up to tens of nanometers have already been synthesized, at low temperature, on functional substrates. Fabrication of nano-systems with a controlled intrinsic gap is a challenge that can have its response in plasma-assisted processes, with the advantage of low temperature and direct growth on desired substrates. In this respect, the seeded growth can be an interesting alternative for high-quality and performance nano-graphene layers with applications in several fields. Also, the use of nano-meshes might be of major interest. Nevertheless, very high complex processes with important economic implications are involved.

Received: March 7, 2013
Revised: July 1, 2013

[1] A. K. Geim, K. S. Novoselov, *Nat. Mater.* **2007**, *6*, 183.
[2] K. S. Novoselov, *Science* **2004**, *306*, 666.
[3] K. S. Novoselov, D. Jiang, F. Schedin, T. J. Booth, V. V. Khotkevich, S. V. Morozov, A. K. Geim, *Prod. Natl. Acad. Sci. USA* **2005**, *102*, 10451.
[4] A. K. Geim, *Science* **2009**, *324*, 1530.
[5] P. R. Somani, S. P. Somani, M. Umeno, *Chem. Phys. Lett.* **2006**, *430*, 56.
[6] X. Li, W. Cai, J. An, S. Kim, J. Nah, D. Yang, R. Piner, A. Velamakanni, I. Jung, E. Tutuc, S. K. Banerjee, L. Colombo, R. S. Ruoff, *Science* **2009**, *324*, 1312.
[7] S. Bae, H. Kim, Y. Lee, X. Xu, J.-S. Park, Y. Zheng, J. Balakrishnan, T. Lei, H. R. Kim, Y. I. Song, Y. Kim, K. S. Kim, B. Özyilmaz, J. H. Ahn, B. H. Hong, S. Iijima, *Nat. Nanotechnol.* **2010**, *5*, 574.
[8] T. Kobayashi, M. Bando, N. Kimura, K. Shimizu, K. Kadono, N. Umezu, K. Miyahara, S. Hayazaki, S. Nagai, Y. Mizuguchi, Y. Murakami, D. Hobara, *Appl. Phys. Lett.* **2013**, *102*, 023112.
[9] A. H. Castro Neto, F. Guinea, N. M. R. Peres, K. S. Novoselov, A. K. Geim, *Rev. Mod. Phys.* **2009**, *81*, 109.
[10] A. Lherbier, S. M.-M. Dubois, X. Declerck, Y.-M. Niquet, S. Roche, J.-C. Charlier, *Phys. Rev. B* **2012**, *86*, 075402.
[11] X. Huang, X. Qi, F. Boeyab, H. Zhang, *Chem. Soc. Rev.* **2012**, *41*, 666.
[12] X. Huang, Z. Yin, S. Wu, X. Qi, Q. He, Q. Zhang, Q. Yan, F. Boey, H. Zhang, *Small* **2011**, *7*, 1876.
[13] M. Inagaki, Y. A. Kim, M. Endo, *J. Mater. Chem.* **2011**, *21*, 3280.
[14] C. Mattevi, H. Kima, M. Chhowalla, *J. Mater. Chem.* **2010**, *20*, 1039.
[15] V. Singh, D. Joung, L. Zhai, S. Das, S. I. Khondaker, S. Seal, *Prog. Mater. Sci.* **2011**, *56*, 1178.
[16] W. Choi, I. Lahiri, R. Seelaboyina, Y. S. Kang, *Crit. Rev. Solid State Mater. Sci.* **2010**, *35*, 52.
[17] Y. Zhang, L. Zhang, C. Zhou, *Acc. Chem. Res.* **2013**, *46*, 2329.
[18] A. Sherman, *Chemical Vapor Deposition for Microelectronics*, Noyes Publications, Park Ridge, NJ **1982**.
[19] H. O. Pierson, *Handbook of Chemical Vapour Deposition*, Noyes Publications, Park Ridge, NJ **1992**.
[20] L. Huimin, *Diamond Chemical Vapour Deposition*, Noyes Publications, Park Ridge, NJ **1995**.

[21] D. S. Rickerby, *Advanced Surface Coatings*, Blackie and Son Ltd, Glasgow, UK **1991**.
[22] K. K. Schuegraf, *Handbook of Thin-film Deposition Processes and Techniques*, Noyes Publications, Park Ridge, NJ **1988**.
[23] J. M. Albella, *Láminas Delgadas y Recubrimientos. Preparación, propiedades y aplicaciones*, CSIC, Spain **2003**.
[24] P. Lenzsolomun, M. C. Wu, W. Goodman, *Catal. Lett.* **1994**, *25*, 75.
[25] A. Reina, X. Jia, J. Ho, D. Nezich, H. Son, V. Bulovic, M. S. Dresselhaus, J. Kong, *Nano Lett.* **2009**, *9*, 30.
[26] K. S. Kim, Y. Zhao, H. Jang, S. Y. Lee, J. M. Kim, K. S. Kim, J. H. Ahn, P. Kim, J. Y. Choi, B. H. Hong, *Nat. Lett.* **2009**, *457*, 706.
[27] X. Li, W. Cai, L. Colombo, R. S. Ruoff, *Nano Lett.* **2009**, *9*, 4268.
[28] M. Kalbac, O. Frank, L. Kavan, *Carbon* **2012**, *50*, 3682.
[29] J. M. Wofford, S. Nie, K. F. McCarty, N. C. Bartelt, O. D. Dubon, *Nano Lett.* **2010**, *10*, 4890.
[30] W. Liu, H. Li, C. Xu, Y. Khatami, K. Banerjee, *Carbon* **2011**, *49*, 4122.
[31] X. Li, C. W. Magnuson, A. Venugopal, J. An, J. Won Suk, B. Han, M. Borysiak, W. Cai, A. Velamakanni, Y. Zhu, L. Fu, E. M. Vogel, E. Voelkl, L. Colombo, R. S. Ruoff, *Nano Lett.* **2010**, *10*, 4328.
[32] M. Losurdo, M. M. Giangregorio, P. Capezzuto, G. Bruno, *Phys. Chem. Chem. Phys.* **2011**, *13*, 20836.
[33] E. M. Sacris, N. A. D. Parlee, *Metall. Mater. Trans. B*, **1970**, *1*, 3377.
[34] W. An, X. C. Zeng, C. H. Turner, *J. Surf. Chem. Phys.* **2009**, *131*, 174702.
[35] W. Zhang, P. Wu, Z. Li, J. Yang, *J. Phys. Chem.* **2011**, *115*, 17782.
[36] C.-T. Au, C.-F. Ng, M.-S. Liao, *J. Catal.* **1999**, *185*, 12.
[37] H. Chen, W. Zhu, Z. Zhang, *Phys. Rev. Lett.* **2010**, *104*, 186101.
[38] S. Riikonen, A. V. Krasheninnikov, L. Halonen, R. M. Nieminen, *J. Phys. Chem. C.* **2012**, *116*, 5802.
[39] G. Jones, F. Studt, F. Abild-Pedersen, J. K. Nørskov, T. Bligaard, *Chem. Eng. Sci.* **2011**, *66*, 6318.
[40] J. W. Medlin, M. D. Allendorf, *J. Phys. Chem. B.* **2003**, *107*, 217.
[41] H. Öberg, Y. Nestsiarenka, A. Matsuda, J. Gladh, T. Hansson, L. G. M. Pettersson, H. Öström, *J. Phys. Chem. C.* **2012**, *116*, 9550.
[42] L.-Q. Lee, D.-H. Shi, Y.-J. Zhao, P.-L. Cao, *J. Phys. Condens. Matter.* **1995**, *7*, 6449.
[43] M. Witko, K. Hermann, *Appl. Catal. A* **1998**, *172*, 85.
[44] O. Skibbe, D. Vogel, M. Binder, A. Pucci, T. Kravchuk, L. Vattuone, V. Venugopal, A. Kokalj, M. Rocca, *J. Chem. Phys.* **2009**, *131*, 024701.
[45] A. V. Zeigarnik, R. E. Valdés-Pérez, O. N. Myatkovskaya, *J. Phys. Chem. B.* **2000**, *104*, 10578.
[46] J. Greeley, M. Mavrikakis, *J. Phys. Chem. B.* **2005**, *109*, 3460.
[47] G. Henkelman, A. Arnaldsson, H. Jónsson, *J. Chem. Phys.* **2006**, *124*, 044706.
[48] G.-C. Wang, J. Nakamura, *J. Phys. Chem. Lett.* **2010**, *1*, 3053.
[49] D. W. Blaylock, T. Ogura, W. H. Green, G. J. O. Beran, *J. Phys. Chem. C.* **2009**, *113*, 4898.
[50] N. M. Galea, D. Knapp, T. Ziegler, *J. Catal.* **2007**, *247*, 20.
[51] P. Wu, W. Zhang, Z. Li, J. Yang, J. G. Hou, *J. Chem. Phys.* **2010**, *133*, 071101.
[52] N. R. Avery, *J. Am. Chem. Soc.* **1985**, *107*, 6711.
[53] T. S. Marinova, P. K. Stefanov, *Surf. Sci.* **1987**, *191*, 66.
[54] J. Gao, J. Zhao, F. Ding, *J. Am. Chem. Soc.* **2012**, *134*, 6204.
[55] Z. Sun, Z. Yan, J. Yao, E. Beitler, Y. Zhu, J. M. Tour, *Nature* **2010**, *468*, 549.
[56] Y.-R. Luo, *Comprehensive Handbook of Chemical Bond Energies*, CRC Press, Boca Raton, FL **2007**, p. 9.
[57] I. Vlassiouk, M. Regmi, P. Fulvio, S. Dai, P. Datskos, G. Eres, S. Smirnov, *ACS Nano* **2011**, *5*, 6069.
[58] L. Gao, W. Ren, J. Zhao, L. P. Ma, Z. Chen, H. M. Cheng, *Appl. Phys. Lett.* **2010**, *97*, 183109.
[59] X. Li, C. W. Magnuson, A. Venugopal, R. M. Tromp, J. B. Hannon, E. M. Vogel, L. Colombo, R. S. Ruoff, *J. Am. Chem. Soc.* **2011**, *133*, 2816.
[60] G. Ruan, Z. Sun, Z. Peng, J. M. Tour, *ACS Nano.* **2011**, *5*, 7601.
[61] T. Wu, G. Ding, H. Shen, H. Wang, L. Sun, D. Jiang, X. Xie, M. Jiang, *Adv. Funct. Mater.* **2013**, *23*, 198.
[62] J. Hofrichter, B. N. Szafranek, M. Otto, T. J. Echtermeyer, M. Baus, A. Majerus, V. Geringer, M. Ramsteiner, H. Kurz, *Nano Lett.* **2010**, *10*, 36.
[63] A. Reina, S. Thiele, X. Jia, S. Bhaviripudi, M. S. Dresselhaus, J. A. Schaefer, J. Kong, *Nano Res.* **2009**, *2*, 509.
[64] B. Zhang, W. Lee, R. Piner, I. Kholmanov, Y. Wu, H. Li, H. Ji, R. S. Ruoff, *ACS Nano* **2012**, *6*, 2471.
[65] B. Hu, H. Ago, C. M. Orofeo, Y. Ogawa, M. Tsujib, *New J. Chem.* **2012**, *36*, 73.
[66] K. S. Kim, Y. Zhao, H. Jang, S. Y. Lee, J. M. Kim, K. S. Kim, J.-H. Ahn, P. Kim, J.-Y. Choi, B. H. Hong, *Nature* **2009**, *457*, 706.
[67] S.-Y. Kwon, C. V. Ciobanu, V. Petrova, V. B. Shenoy, J. Bare∼no, V. Gambin, I. Petrov, S. Kodambaka, *Nano Lett.* **2009**, *9*, 3985.
[68] Z. Yan, J. Lin, Z. Peng, Z. Sun, Y. Zhu, L. Li, C. Xiang, E. L. Samuel, C. Kittrell, J. M. Tour, *ACS Nano* **2012**, *6*, 9110.
[69] S. Chen, H. Ji, H. Chou, Q. Li, H. Li, J. Won Suk, R. Piner, L. Liao, W. Cai, R. S. Ruoff, *Adv. Mater.* **2013**, *25*, 2062.
[70] E. Loginova, N. C. Bartelt, P. J. Feibelman, K. F. McCarty, *New J. Phys.* **2009**, *11*, 063046.
[71] L. Gao, W. Ren, H. Xu, L. Jin, Z. Wang, T. Ma, L.-P. Zhiyong Zhang, Q. Fu, L.-M. Peng, X. Bao, H.-M. Cheng, *Nat. Commun.* **2012**, *3*, 699.
[72] A. Earnshaw, T. J. Harrington, *The Chemistry of Transition Elements*, Clarendon Press, Oxford **1973**.
[73] J. Hou, Y. Shao, M. W. Ellis, R. B. Moored, B. Yie, *Phys. Chem. Chem. Phys.* **2011**, *13*, 15384.
[74] A. N. Obraztsov, E. A. Obraztsova, A. V. Tyurnina, A. A. Zolotukhin, *Carbon* **2007**, *45*, 2017.
[75] A. Umair, H. Raza, *Nanoscale Res. Lett.* **2012**, *7*, 437.
[76] Y. Xue, B. Wu, Y. Guo, L. Huang, L. Jiang, J. Chen, D. Geng, Y. Liu, W. Hu, G. Yu, *Nano Res.* **2011**, *4*, 1208.
[77] M. Zheng, K. Takei, B. Hsia, H. Fang, X. Zhang, N. Ferralis, H. Ko, Y.-L. Chueh, Y. Zhang, R. Maboudian, A. Javey, *Appl. Phys. Lett.* **2010**, *96*, 063110.
[78] S. Chen, W. Cai, R. D. Piner, J. Won Suk, Y. Wu, Y. Ren, J. Kang, R. S. Ruoff, *Nano Lett.* **2011**, *11*, 3519.
[79] Z. R. Robinson, P. Tyagi, T. M. Murray, C. A. Ventrice, Jr, S. Chen, A. Munson, C. W. Magnuson, R. S. Ruoff, *J. Vac. Sci. Technol. A* **2012**, *30*, 011401.
[80] T. Sakurai, T. Hashizume, A. Kobayashi, A. Sakai, S. Hyodo, Y. Kuk, H. W. Pickering, *Phys. Rev. B.* **1986**, *34*, 8379.
[81] X. Liu, L. Fu, N. Liu, T. Gao, Y. Zhang, L. Liao, Z. Liu, *J. Phys. Chem. C.* **2011**, *115*, 11976.
[82] R. S. Weatherup, B. C. Bayer, R. Blume, C. Ducati, C. Baehtz, R. Schlogl, S. Hofmann, *Nano Lett.* **2011**, *11*, 4154.
[83] S. K. Jerng, D. S. Yu, Y. S. Kim, J. Ryou, S. Hong, C. Kim, S. Yoon, D. K. Efetov, P. Kim, S. H. Chun, *J. Phys. Chem. C.* **2011**, *115*, 4491.
[84] K. B. Kim, C. M. Lee, J. Choi, *J. Phys. Chem. C.* **2011**, *115*, 14488.
[85] C. M. Lee, J. Choi, *Appl. Phys. Lett.* **2011**, *98*, 183106.
[86] L. Zhang, Z. Shi, Y. Wang, R. Yang, D. Shi, G. Zhang, *Nano Res.* **2011**, *4*, 315.
[87] X. Ding, G. Ding, X. Xie, F. Huang, M. Jiang, *Carbon* **2011**, *49*, 2522.
[88] M. H. Rummeli, A. Bachmatiuk, A. Scott, F. Borrnert, J. H. Warner, V. Hoffman, J. H. Lin, G. Cuniberti, B. Beuchner, *ACS Nano* **2010**, *4*, 4206.
[89] H. Bi, F. Q. Huang, J. Liang, X. M. Xie, M. H. Jiang, *Adv. Mater.* **2011**, *23*, 3202.
[90] H. Bi, S. Sun, F. Huang, X. Xieb, M. Jiang, *J. Mater. Chem.* **2012**, *22*, 411.
[91] A. Ismach, C. Druzgalski, S. Penwell, A. Schwartzberg, M. Zheng, A. Javey, J. Bokor, Y. Zhang, *Nano Lett.* **2010**, *10*, 1542.
[92] K. Kim, Z. Lee, W. Regan, C. Kisielowski, M. F. Crommie, A. Zettl, *ACS Nano* **2011**, *5*, 2142.
[93] L. Gao, J. R. Guest, N. P. Guisinger, *Nano Lett.* **2010**, *10*, 3512.
[94] L. Zhao, K. T. Rim, H. Zhou, R. He, T. F. Heinz, A. Pinczuk, G. W. Flynn, A. N. Pasupathy, *Solid State Commun.* **2011**, *151*, 509.
[95] J. D. Wood, S. W. Schmucker, A. S. Lyons, E. Pop, J. W. Lyding, *Nano Lett.* **2011**, *11*, 4547.
[96] W. Zhang, P. Wu, Z. Li, J. Yang, *J. Phys. Chem. C.* **2011**, *115*, 17782.
[97] D. Chatain, V. Ghetta, P. Wynblatt, *Interface Sci.* **2004**, *12*, 7.
[98] H. Ago, Y. Ito, N. Mizuta, K. Yoshida, B. Hu, C. M. Orofeo, M. Tsuji, K. Ikeda, S. Mizuno, *ACS Nano* **2010**, *4*, 7407.
[99] T. Iwasaki, H. J. Park, M. Konuma, D. S. Lee, J. H. Smet, U. Starke, *Nano Lett.* **2011**, *11*, 79.
[100] B. Hu, H. Ago, Y. Ito, K. Kawahara, M. Tsuji, E. Magome, K. Sumitani, N. Mizuta, K. Ikeda, S. Mizuno, *Carbon* **2012**, *50*, 57.
[101] K. M. Reddy, A. D. Gledhill, C. H. Chen, J. M. Drexler, N. P. Padturea, *Appl. Phys. Lett.* **2011**, *98*, 113117.
[102] C. V. Van, A. Kimouche, A. R. Plantey, O. Fruchart, P. B. Guillemaud, N. Bendiab, J. Coraux, *J. Appl. Phys. Lett.* **2011**, *98*, 181903.
[103] P. W. Sutter, P. M. Albrecht, E. A. Sutter, *Appl. Phys. Lett.* **2010**, *97*, 213101.
[104] S. Yoshii, K. Nozawa, K. Toyoda, N. Matsukawa, A. Odagawa, A. Tsujimura, *Nano Lett.* **2011**, *11*, 2628.
[105] Y. Ogawa, B. Hu, C. M. Orofeo, M. Tsuji, K. Ikeda, S. Mizuno, H. Hibino, H. Ago, *J. Phys. Chem. Lett.* **2012**, *3*, 219.

[106] M. P. Levendorf, C. S. Ruiz-Vargas, S. Garg, J. Park, *Nano Lett.* **2009**, *9*, 4479.
[107] C. A. Howsare, X. Weng, V. Bojan, D. Snyder, J. A. Robinson, *Nanotechnology* **2012**, *23*, 135601.
[108] J. Kedzierski, P.-L. Hsu, A. Reina, J. Kong, P. Healey, P. Wyatt, C. Keast, *IEEE Electron Device Lett.* **2009**, *30*, 745.
[109] Z. Luo, Y. Lu, D. W. Singer, M. E. Berck, L. A. Somers, B. R. Goldsmith, A. T. C. Johnson, *Chem. Mater.* **2011**, *23*, 1441.
[110] O. V. Yazyev, A. Pasquarello, *Phys. Rev. Lett.* **2008**, *100*, 156102.
[111] S. Saadi, F. Abild-Pedersen, S. Helveg, J. Sehested, B. Hinnemann, C. C. Appel, J. K. Nørskov, *J. Phys. Chem. C.* **2010**, *114*, 11221.
[112] S. Helveg, C. López-Cartes, J. Sehested, P. L. Hansen, B. S. Clausen, J. R. Rostrup-Nielsen, F. Abild-Pedersen, J. K. Nørskov, *Nature* **2004**, *427*, 426.
[113] F. Abild-Pedersen, J. K. Nørskov, J. R. Rostrup-Nielsen, S. Sehested, S. Helveg, *Phys. Rev. B.* **2006**, *73*, 115419.
[114] H. Bengaard, J. K. Nørskov, J. Sehested, B. S. Clausen, L. P. Nielsen, A. M. Molenbroek, J. R. Rostrup-Nielsen, *J. Catal.* **2002**, *209*, 365.
[115] S. Nie, J. M. Wofford, N. C. Bartelt, O. D. Dubon, K. F. McCarty, *Phys. Rev. B* **2011**, *84*, 155425.
[116] E. Sutter, P. Albrecht, P. Sutter, *Appl. Phys. Lett.* **2009**, *95*, 133109.
[117] P. Y. Huang, C. S. Ruiz-Vargas, A. M. van der Zande, W. S. Whitney, M. P. Levendorf, J. W. Kevek, S. Garg, J. S. Alden, C. J. Hustedt, Y. Zhu, J. Park, P. L. McEuen, D. A. Muller, *Nature* **2011**, *469*, 391.
[118] F. Jansen, M. A. Machonkin, D. E. Kuhman, *J. Vac. Sci. Technol. A* **1990**, *8*, 3785.
[119] Q. K. Yu, L. A. Jauregui, W. Wu, R. Colby, J. F. Tian, Z. H. Su, H. L. Cao, Z. H. Liu, D. Pandey, D. G. Wei, T. F. Chung, P. Peng, N. Guisinger, E. A. Stach, J. M. Bao, S. S. Pei, Y. P. Chen, *Nat. Mater.* **2011**, *10*, 443.
[120] W. Wu, L. A. Jauregui, Z. Su, Z. Liu, J. Bao, Y. P. Chen, Q. Yu, *Adv. Mater.* **2011**, *23*, 4898.
[121] S. Bhaviripudi, X. Jia, M. S. Dresselhaus, J. Kong, *Nano Lett.* **2010**, *10*, 4128.
[122] A. W. Robertson, J. H. Warner, *Nano Lett.* **2011**, *11*, 1182.
[123] W. Wu, Q. Yu, P. Peng, Z. Liu, J. Bao, Shin-S. Pei, *Nanotechnology* **2012**, *23*, 035603.
[124] T. Kaplas, D. Sharma, Y. Svirko, *Carbon* **2012**, *50*, 1503.
[125] Y. Zhang, L. Zhang, P. Kim, M. Ge, Z. Li, C. Zhou, *Nano Lett.* **2012**, *12*, 2810.
[126] H. Wang, G. Wang, P. Bao, S. Yang, W. Zhu, X. Xie, W.-J. Zhang, *J. Am. Chem. Soc.* **2012**, *134*, 3627.
[127] Y. Zhang, Z. Li, P. Kim, L. Zhang, C. Zhou, *ACS Nano* **2012**, *6*, 126.
[128] L. Huang, Q. H. Chang, G. L. Guo, Y. Liu, Y. Q. Xie, T. Wang, B. Ling, H. F. Yang, *Carbon* **2012**, *50*, 551.
[129] Z. Y. Juang, C. Y. Wu, A. Y. Lu, C. Y. Su, K. C. Leou, F. R. Chen, *Carbon* **2010**, *48*, 3169.
[130] H. J. Park, J. Meyer, S. Roth, V. Skakalova, *Carbon* **2010**, *48*, 1088.
[131] E. Fromm, H. Jehn, *Bull. Alloy Phase Diagrams.* **1984**, *5*, 324.
[132] D. Geng, B. Wu, Y. Guo, L. Huang, Y. Xue, J. Chen, G. Yu, L. Jiang, W. Hu, Y. Liu, *Proc. Natl. Acad. Sci. USA* **2012**, *109*, 7992.
[133] B. Wu, *Adv Mater.* **2011**, *23*, 3522-.
[134] K. S. Novoselov, V. I. Falko, L. Colomo, P. R. Gellert, M. G. Schwab, K. Kim, *Nature* **2012**, *490*, 192.
[135] J. Kim, M. Ishihara, Y. Koga, K. Tsugawa, M. Hasegawa, S. Iijima, *Appl. Phys. Lett.* **2011**, *98*, 091502.
[136] Y. Kim, W. Song, S. Y. Lee, C. Jeon, W. Jung, M. Kim, C.-Y. Park, *Appl. Phys. Lett.* **2011**, *98*, 263106.
[137] T. Terasawa, K. Saiki, *Carbon* **2012**, *50*, 869.
[138] J. L. Qi, L. X. Zhang, J. Cao, *Chin. Sci. Bull.* **2012**, *57*, 3040.
[139] G. Kalita, M. S. Kayastha, H. Uchida, K. Wakita, M. Umeno, *RSC Adv.* **2012**, *2*, 3225.
[140] A. Kumar, A. A. Voevodin, D. Zemlyanov, D. N. Zakharov, T. S. Fisher, *Carbon* **2012**, *50*, 1546.
[141] Q. Yu, J. Lian, S. Siriponglert, H. Li, Y. P. Chen, S.-S. Pei, *Appl. Phys. Lett.* **2008**, *93*, 113103.
[142] S. Lee, K. Lee, Z. Zhong, *Nano Lett.* **2010**, *10*, 4702.
[143] J. Gao, J. Yip, J. Zhao, B. I. Yakobson, F. J. Ding, *J. Am. Chem. Soc.* **2011**, *133*, 5009.
[144] H. H. Angermann, Z. Horz, *Appl. Surf. Sci.* **1993**, *70*, 163.
[145] H. Bi, F. Huang, W. Zhao, X. Lu, J. Chen, T. Lin, D. Wan, X. Xie, M. Jiang, *Carbon* **2012**, *50*, 2703.
[146] T. Yamada, M. Ishihara, J. Kim, M. Hasegawa, S. Iijima, *Carbon* **2012**, *50*, 2615.
[147] T. Ohta, A. Bostwick, T. Seyller, K. Horn, E. Rotenberg, *Science* **2006**, *313*, 951.
[148] K. Yan, H. Peng, Y. Zhou, H. Li, Z. Liu, *Nano Lett.* **2011**, *11*, 1106.
[149] X. Li, X. Wang, L. Zhang, S. Lee, H. Dai, *Science* **2008**, *319*, 1229.
[150] D. V. Kosynkin, W. Lu, A. Sinitskii, G. Pera, Z. Sun, J. M. Tour, *ACS Nano* **2011**, *5*, 968.
[151] J. Bai, X. Zhong, S. Jiang, Y. Huang, X. Duan, *Nat. Nanotechnol.* **2010**, *5*, 190.
[152] M. Wang, L. Fu, L. Gan, C. Zhang, M. Rümmeli, A. Bachmatiuk, K. Huang, Y. Fang, Z. Liu, *Sci. Rep.* **2013**, *3*, 1238.
[153] J. J. Wang, M. Y. Zhu, R. A. Outlaw, X. Zhao, D. M. Manos, *Appl. Phys. Lett.* **2004**, *85*, 1265.
[154] A. Malesevic, R. Vitchev, K. Schouteden, A. Volodin, L. Zhang, G. Van Tendeloo, A. Vanhulsel, C. Van Haesendonck, *Nanotechnology* **2008**, *19*, 305604.
[155] C. Y. Cheng, K. Teii, *IEEE Trans. Plasma Sci.* **2012**, *40*, 1783.
[156] C.-H. Tu, W. Chen, H.-C. Fang, Y. Tzeng, C.-P. Liu, *Carbon* **2013**, *54*, 234.
[157] L. Jiao, X. Wang, G. Diankov, H. Wang, H. Dai, *Nat. Nanotechnol.* **2010**, *5*, 321.
[158] Y. S. Zhou, W. Xiong, J. Park, M. Qian, M. Mahjouri-Samani, Y. Gao, L. Jiang, Y. Lu, *J. Laser Appl.* **2012**, *24*, 042007.

